

AD 708 699
66 80 207

T-WAVE GENERATION MECHANISMS

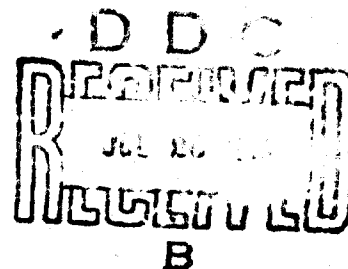
By
ROCKNE H. JOHNSON
and
ROGER A. NORRIS

JANUARY 1970

FINAL REPORT

Prepared for

ADVANCED RESEARCH PROJECTS AGENCY
UNDER CONTRACT NO. Nonr-3748(01)
ARPA ORDER NO. 218 AMENDMENT 7
PROJECT CODE 8100



HAWAII INSTITUTE OF GEOPHYSICS
UNIVERSITY OF HAWAII



This document has been approved
for public release and sale; its
distribution is unlimited.

63

T-WAVE GENERATION MECHANISMS

By

Rockne H. Johnson

and

Roger A. Norris

January 1970

FINAL REPORT

Prepared for

Advanced Research Projects Agency
under Contract No. Nonr-3748(01)
ARPA Order No. 218 Amendment 7
Project Code 8100

Reproduction of this report in whole or in part is permitted
for any purpose of the United States Government

Approved by Director

A handwritten signature in dark ink, appearing to read "George V. Skelland", is written over the "Approved by Director" line.

Date: 10 February 1970

Contents

	<u>Page</u>
Abstract	1
Introduction	3
Background	3
Data	4
Deep-Slope <u>T</u> Waves	4
Propagation of Deep-Slope <u>T</u> Waves	9
Abyssal <u>T</u> Waves	10
Conclusion	13
Acknowledgments.	14
References	15
Appendix	A-1

ABSTRACT

The transformation of earthquake body waves to T waves is as efficient at deep slopes as at slopes which transect the sofar axis. Moreover, spectral studies of T phase signatures have shown no basis for distinguishing between the two cases. As simple downslope propagation is inadequate to explain the production of T waves at deep slopes, that process is relegated a minor role in favor of scattering from the sea floor as the dominant mechanism. A slope in the direction of propagation insures that once energy is scattered in that direction the probability of its being unfavorably rescattered upon successive approaches to the sea floor will be less. Scattering near the sea surface is detectable in the absence of bottom-scattered T waves. Such abyssally generated T waves display a distinctly higher frequency spectrum when originating in subarctic regions than when originating in lower latitudes. This difference is ascribed to downward ducting of higher frequency energy from the subarctic surface channel.

INTRODUCTION

A widely recognized gap in extant hypotheses for the generation of T waves is the explanation of the strong signals received from the East Pacific Rise. There the ocean is too deep to support the production of sofar rays by downslope propagation. The T phases received, however, resemble those generated at shallow slopes much more closely than those generated at abyssal depths (i.e., in close proximity to trenches). A second problem is the observed difference between the spectrum of abyssal T waves generated in the subarctic and that of T waves from lower latitudes. In order to resolve these problems a study has been conducted of sonagrams (intensity level contoured in the frequency-time plane) of T phases from over 400 earthquakes occurring all around the Pacific.

BACKGROUND

Tolstoy and Ewing (1950) recognized the importance of a sloping bottom in the production of T waves. The specific mechanism of multiple reflection between the sea surface and its downsloping bottom (downslope propagation) was first detailed by Milne (1959). Johnson et al. (1963) showed that, for a 10° slope and an acoustic profile typical of the Aleutians, the downslope propagation process would produce sound channel rays only if the rays entered the water at depths of less than about 500 meters. For RSR (refracted surface-reflected) rays this limiting depth is perhaps doubled. Although T waves originating over ocean trenches have been observed, their spectral and time-varying characteristics differ markedly from slope T waves and a generative mechanism involving scattering at the sea surface has been proposed (Johnson et al., 1968). These authors noted, however, that T phases originating along the East Pacific Rise display the low-frequency spectrum of slope T phases, yet the

waves cannot be accounted for by downslope propagation. Cooke (1967) also recognized this predicament. It is necessary, then, to modify the hypothesis for slope T-phase generation to include T phases generated at deeper slopes.

DATA

The data presented in the appendix to this report are sonagrams made from over 400 earthquake T phases tape-recorded from sound-channel hydrophones of the Pacific Missile Range at Oahu, Midway, Wake, and Eniwetok islands. Tapes were ordered for analysis if the paper-drum recordings from the stations contained T phases from earthquakes which were identified by the U. S. Coast and Geodetic Survey (C&GS) preliminary determination of epicenter cards as being from abyssal regions or from an earthquake of magnitude 6 or greater. In processing the tapes, every T phase generated by an earthquake identified by the C&GS was sonagrammed irrespective of magnitude or region. No attempt was made to compensate for the response of the hydrophone-cable-amplifier systems, although their characteristics vary from installation to installation and systematic spectral differences are thereby introduced.

DEEP-SLOPE T WAVES

A verification that T waves are indeed radiated from deep slopes is illustrated by a sequence of earthquakes which occurred off northern Honshu in June 1968. The foci of four of the earthquakes are shown in Figure 1 as well as the focus of an earthquake farther offshore. The source data are listed in Table I. Figure 2 presents the sonagrams of the corresponding T phases. (Frequency

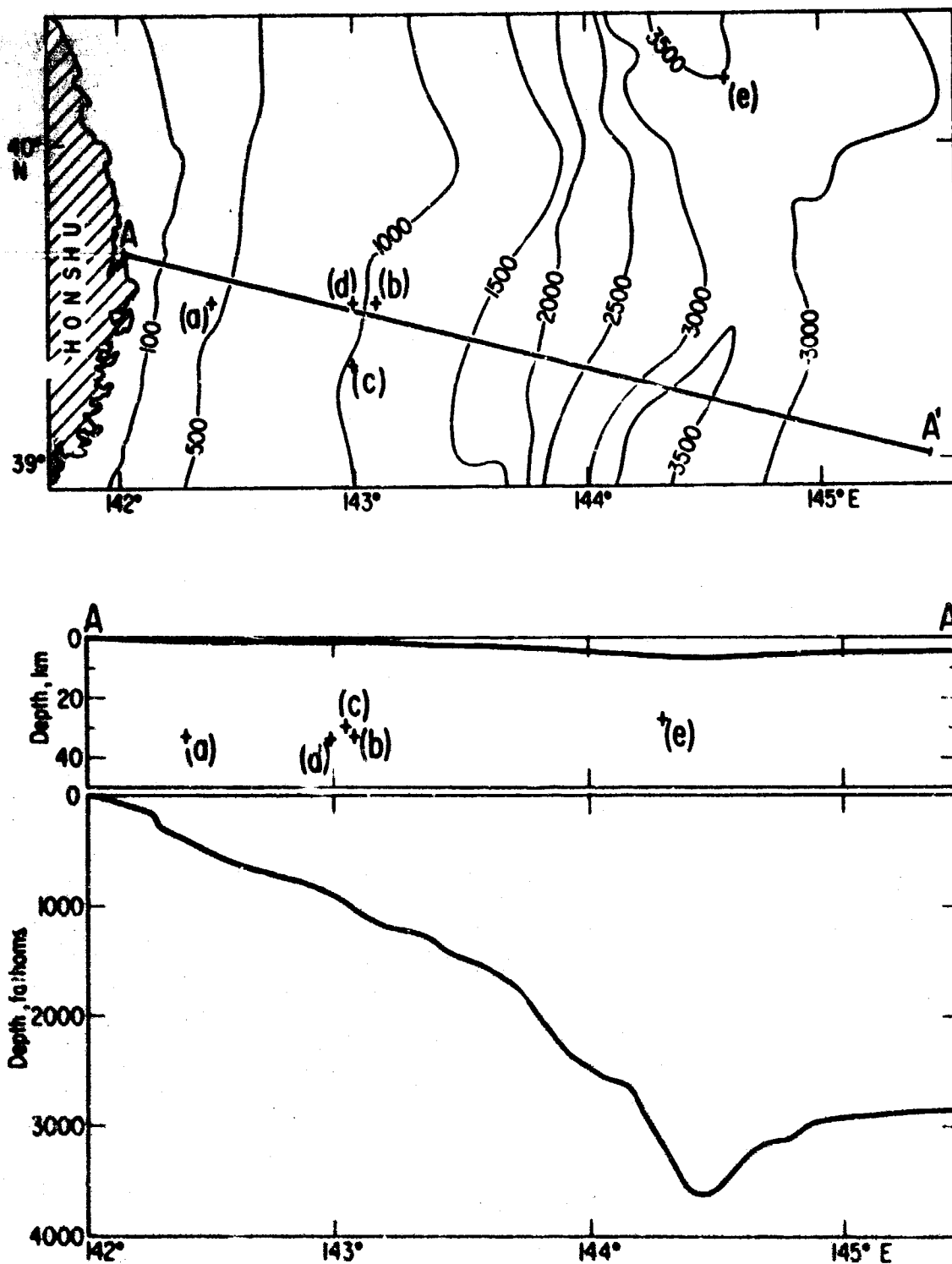


Fig. 1. The foci of five earthquakes off northern Honshu shown both in plan (upper) and elevation (lower). Bottom contours are in fathoms. Source data are listed in Table I and sonagrams are presented in Figure 2. The bathymetry along section A-A' is shown both true scale and with 20X vertical exaggeration.

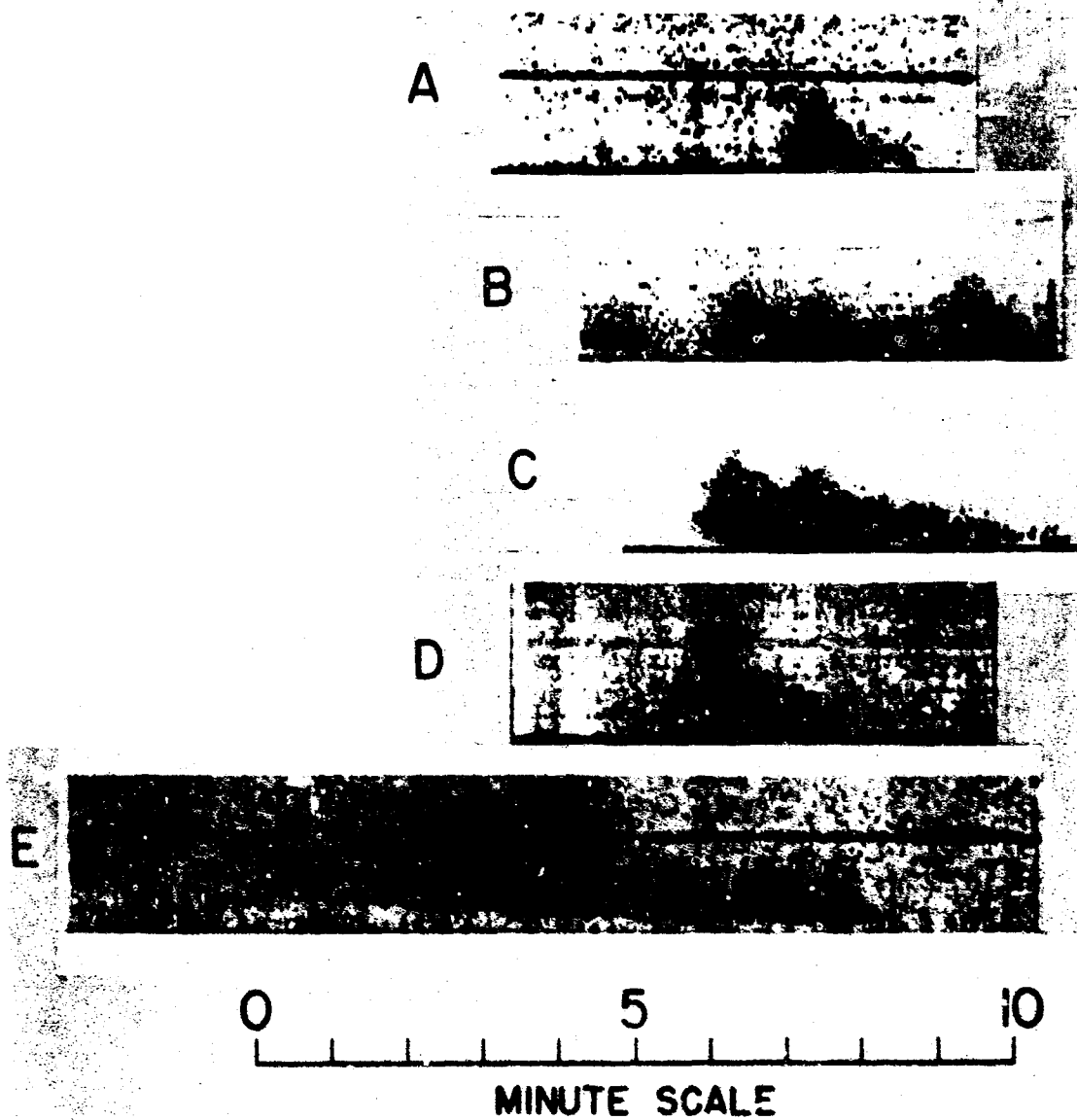


FIG. 2. Sonograms of *T* phases from earthquakes off northern Honshu. Foci are shown in Figure 1 and source data are listed in Table 1. (Frequency range is 0 to 50 Hz in these and all other sonograms.)

Table I. Source Data for Events Shown in Figure 1.

Selected Off-Honshu Earthquakes						
Event	Lat., °N	Long., °E	Depth, km	Mag., M _b	Date, d m y	GMT, h m s
a	39.5	142.4	33	4.1	18 Jun 68	13 38 01
b	39.5	143.1	33	4.3	12 Jun 68	17 23 18
c	39.3	143.0	30	5.1	12 Jun 68	15 48 59.5
d	39.5	143.0	34	4.5	26 Jun 68	20 26 19.0
e	40.2	144.6	27	5.0	24 Mar 67	04 11 29.6

range: 0 to 50 h, bottom to top on all sonagrams in this report.) Event (a) is characteristic of slope I phases while event (e) generated both an abyssal and a slope I phase at a spacing appropriate for the distance of the epicenter from the continental shelf. Likewise, events (b), (c), and (d) also generated two groups of I waves, each of which is appropriately spaced for the distance of the epicenter from the shelf. In cases (b), (c), and (d), however, the first group of waves lacks the identifying characteristics of an abyssal I phase, the only notable distinction from the second group being the inclusion of higher frequencies. The water depth at epicenters (b), (c), and (d) was about 2000 meters with a bottom slope of one to two degrees. These conditions are clearly insufficient to produce even RSR rays by downslope propagation over a smooth bottom (Aubrat, 1963).

In fact, however, continental and island slopes are not smooth, but are cut by submarine canyons and crossed by fault scarps which serve to scatter acoustic energy upon initial refraction into the water as well as during multiple reflection within the water wedge. This scattering materially reduces the

length of slope required to produce horizontal rays.

The scattering mechanism is equally operable at shallow slopes and must equally cause the production of shallow-slope I waves. The shallow-slope I phases may be slightly stronger at the lower frequencies however, since longer wavelengths, which are not as readily scattered, can be deflected into horizontal paths by the length of a slope available. The lack of higher frequency energy for the shallow-slope I phases shown in Figure 2 is ascribable to attenuation over the longer ground path. This variation of low-frequency content with water depth was recognized by Duennebie (1968) as a decrease of peak frequency with time over the early portions of slope I phases from the Fox Islands.

Computed sources of slope I phases have been found to form clusters indicative of topographically controlled sites of strong radiation (Johnson and Norris, 1968a; Duennebie and Johnson, 1967). By contrast, abyssal I-phase sources appear to radiate most strongly from the earthquake epicenter. The excitation of a uniform scattering horizon is inferred from the very gradual onset and decay rates of abyssal I waves. The onset and decay rates of deep-slope I waves are practically identical with those of shallow-slope I waves, suggesting a similar topographic control of radiation. The lack of any basis for distinction between the two groups of signals is readily apparent in Figure 3, which contains a selection of sonagrams from earthquakes along the East Pacific Rise as well as a selection of shallow-slope I waves (Table II).

The mechanism and conditions for generation of deep-slope I waves also apply to I waves from the East Pacific Rise. Although here the average slope is much more gradual than at the margins of the Pacific, the topography is characteristically faulted, the faults apparently being in close association with earthquake epicenters. Such fault scarps, then, at once provide the

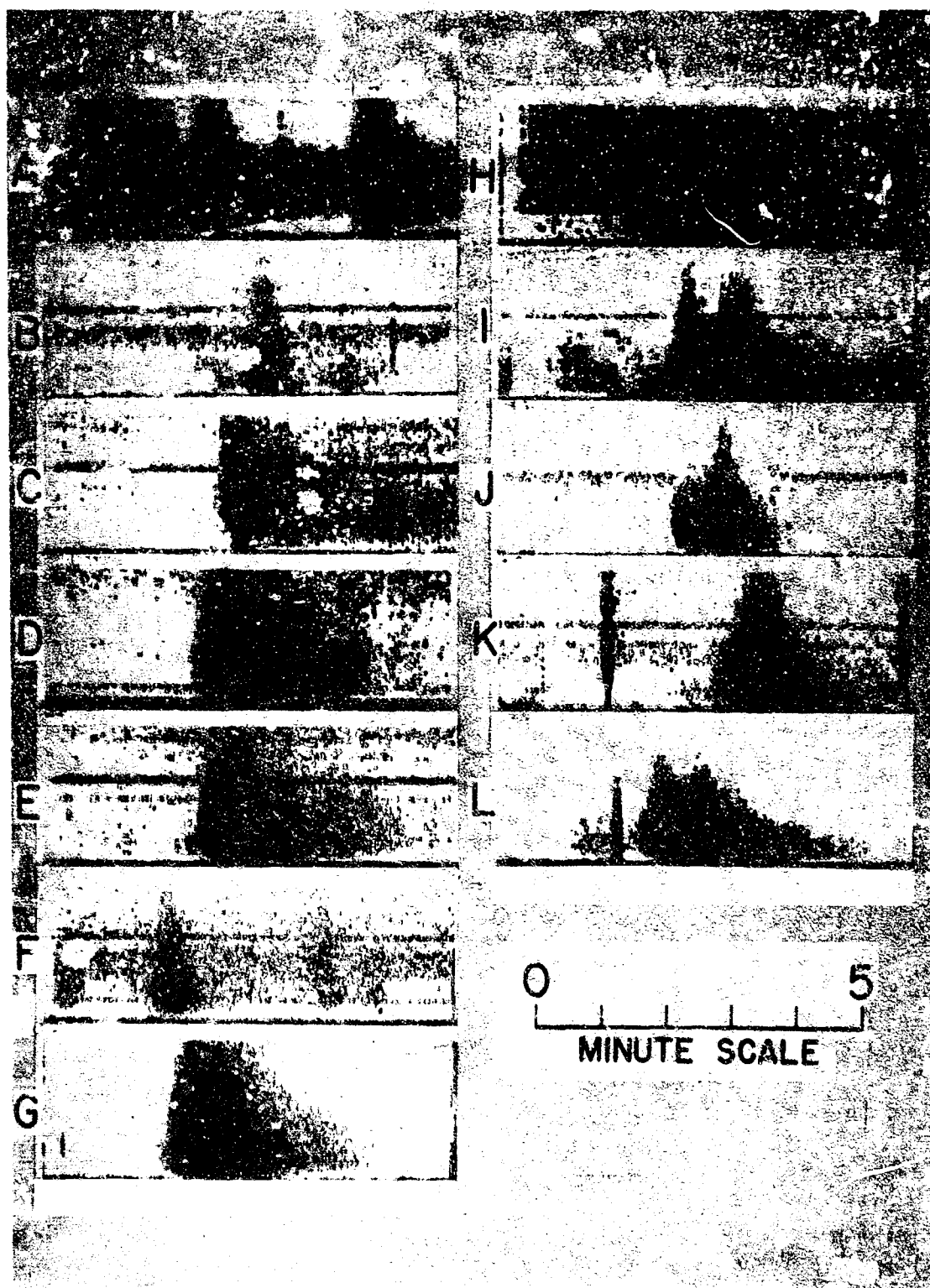


FIG. 3. Selected sonograms of *T* phases from the East Pacific Rise (on the left) and selected shallow-slope *T* phases (on the right). Source data are listed in Table II.

Table II. Source Data for Events Shown in Figure 3.

Selected East Pacific Rise Earthquakes (Fig. 3, left)						
Event	Lat.	Long., °W	Depth, km	Mag., M_b	Date, d m y.	GMT, h m s
a	44.2N	128.8	33	5.4	28 Dec 67	06 26 15.8
b	42.0N	126.2	33	4.9	26 Sep 67	05 51 11
c	2.6N	101.8	33	4.9	28 Mar 68	12 44 38.0
d	2.1N	101.1	33	4.7	30 Dec 67	02 46 55
e	4.0S	104.1	33	4.5	16 Jun 68	14 01 22
f	32.8S	111.7	33	5.4	29 Dec 66	22 16 22.7
g	54.8S	136.0	33	5.4	9 Sep 67	16 52 01.3

Selected Shallow-Slope T Phases (Fig. 3, right)

h	40.6N	125.0	33	4.4	17 Jun 68	03 05 44
i	40.5N	124.6	05	5.8	10 Dec 67	12 06 50.3
j	37.0N	121.8	11	5.0	18 Dec 67	17 24 31.9
k	20.0S	70.3	60	4.6	8 Nov 67	10 47 45.3
l	21.5S	70.4	53	5.8	25 Dec 67	10 41 31.6

scattering facets and the localized radiators for deep-slope T wave generation.

T-phase strength offers no basis for distinguishing between deep-slope and shallow-slope T phases. T phases from the Gorda Ridge (Northrop et al., 1968)--which is well below the seafloor axis--are at least as strong, relative to earthquake magnitude, as slope T phases from the Aleutian Ridge (Johnson and Northrop, 1966;

Johnson and Norris, 1968a). Deep-towed-echosounder profiles of the Gorda Ridge indicate faulted blocks with scarps dipping at 30-degree angles (Atwater and Mudie, 1968). Such rugged terrain probably accounts for strong T-wave generation.

T phases originating along southern portions of the East Pacific Rise are equally as strong as those from the Gorda Ridge. Here the relief along the crest of the rise is more subdued, however earthquake epicenters are found to lie principally along the steep-sided fracture zones which offset the rise (Menard, 1966; Sykes, 1963).

Duennebier (1968), in describing an Eniwetok hydrophone recording of a magnitude 6.2 earthquake under the Mariana Ridge, states that energy was continuously received at the hydrophone from the time of the P phase arrival until after the arrival of the slope T phase from the Mariana Ridge. Strong signals were received at intermediate times, corresponding to P-wave travel to intervening seamounts followed by T-wave travel to the hydrophone. Although, as Duennebier points out, the tops of these seamounts are well below the sofar axis, such steep slopes (Robertson and Kibblewhite, 1966) may be expected to radiate T waves into RSR and off-axis sofar paths with relative efficiency.

Two earthquakes from the North Pacific Basin have their foci (Table III) under the newly discovered Emperor Fracture Zone (Erickson et al., 1970). Here, the bottom is characterized by irregular ridges and troughs with elevations no more than 1 km above the regional level. Since all depths in the epicentral region are greater than the bottom of the sofar channel, only RSR and multiply reflecting rays can be generated by scatter at the sea floor. The T phases recorded at Midway (Figure 4a and b) show the characteristic broad spectrum of such bottom-scattered waves, but in addition they show the gradual onset and decay that is suggestive of a uniform scattering horizon. This effect may be due to the alignment of the topography with the direction to Midway or the

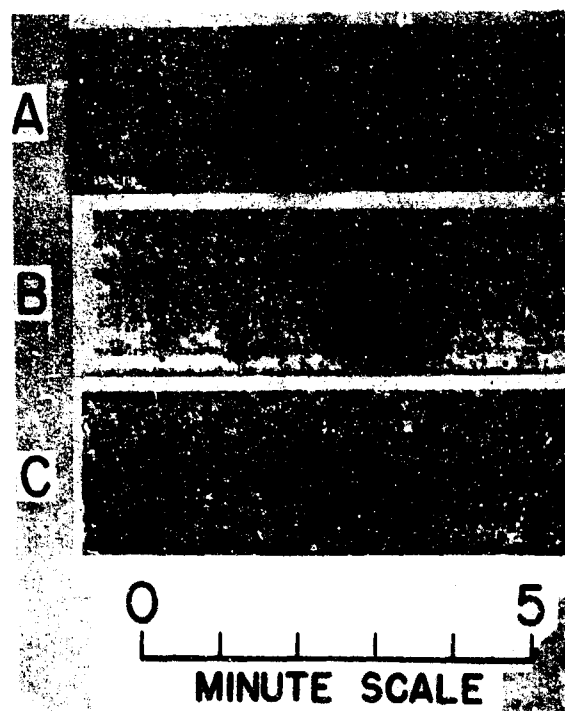


FIG. 4. Sonograms of *T* phases from earthquakes under the deep-ocean floor. Source data are listed in Table III.

result of the superposition of near-surface scattered (abyssal) I waves upon bottom-scattered waves.

Table III. Source Data for Events Shown in Figure 4.

Event	Lat.	Long.	Depth, km	Mag., M_b	Date,			GMT,		
					d	m	y	h	m	s
a	44.8N	174.5E	39	5.5	28	Apr	68	04	18	15.7
b	44.8N	174.7E	33	4.3	28	Apr	68	06	23	02
c	12.0N	130.8W	33	5.3	24	Sep	66	08	57	10.2

Figure 4c shows another Pacific Basin I phase with its focus (Table III) under the less well-charted ocean floor between Clarion and Clipperton fracture zones. The low strength of this I phase, relative to the earthquake magnitude, suggests a lack of topographic relief in the epicentral region.

PROPAGATION OF DEEP-SLOPE I WAVES

RSR paths exist when the speed of sound in the bottom water is greater than it is at the surface. This condition is easily met in higher latitudes where the surface water is cold; but in the tropical and sub-tropical Pacific, existence of the condition depends strongly on water depth. From about 45°N to 40°S the East Pacific Rise is too shallow to permit RSR propagation. Within this region such sound energy as is scattered clear of a sloping bottom will enter the sofar channel as off-axis rays. At higher latitudes proportionately more energy will be scattered into initially RSR paths. Such paths may become totally refracted sofar paths upon entering regions of warmer surface water.

Unattenuated propagation by totally reflecting paths (normal

mode) is theoretically possible in a constant-depth ocean. However, if bottom scattering is an acceptable mechanism for slope T-wave generation, a continuation of that scattering over the travel path would militate against propagation--by normal mode--to significant distances. The very low frequencies at which sound may be effectively propagated by bottom-reflecting normal mode in the deep ocean are beyond the sensing range of presently installed hydrophones.

In computing T-phase source locations, it has been assumed that the most intense arrival travels at sofar-axis sound speed (Johnson, 1966). As no near-axis sofar rays are generated by the proposed deep-slope T-wave mechanism, a somewhat higher apparent sound speed would be appropriate to such cases. For example, in the vicinity of Midway, the sofar ray which is horizontal at a 3000-meter depth has an apparent speed that is 0.3% higher than the speed of the sofar axis ray. Such a difference in speed would produce about an 8-second arrival-time difference over the path from the tropical East Pacific Rise to Midway. This would correspond to a source location difference of .25°. The simple, sharply peaked signature of East Pacific Rise T phases should readily allow the detection of such a discrepancy were the epicenter known with sufficient accuracy. Such is not likely to be the case in this remote region of the Pacific, however.

ABYSSAL T WAVES

Situations where the bottom cannot scatter energy into RSR or sofar paths occur where the ocean floor is level or at a greater depth than adjacent areas in the direction of the receiver. Johnson et al. (1968) detected T waves from such regions in the subarctic Pacific and termed them "abyssally generated". The signals were characterized by very gradual onset, a lack of low frequencies, and

a low strength relative to earthquake magnitude. They usually appear as the forerunner of a slope-generated I phase (Doennebier, 1968).

For Pacific earthquakes in lower latitudes, the forerunners, which may commence at the time for direct P-wave arrival, show no perceptible difference in spectrum from the slope arrivals. Figure 5 illustrates this contrast between the forerunners of subarctic and lower latitude I phases (source data listed in Table IV). As previously noted, the occasional intensification of

Table IV. Source Data for Events Shown in Figure 5.

Event	Lat.	Long.	Depth, km	Mag., M_b	Date,			GMT,		
					d	m	y	h	m	s
a	50.6N	171.3W	39	6.5	7	Aug	66	02	13	05.1
b	44.3N	151.7E	26	5.8	7	Dec	66	17	17	42.0
c	40.8N	143.2E	07	7.9	16	May	68	00	48	55.4
d	27.4N	144.3E	40	4.6	6	Feb.	64	08	00	35.0
e	20.8N	146.3E	43	6.2	10	Feb	66	14	21	10.9
f	18.4N	146.5E	77	5.0	20	Jan	68	20	06	48.0
g	7.1S	81.6W	23	6.5	29	Aug	63	15	30	31.4

signal strength in the lower latitude events may be accounted for by radiation from intervening seamounts. However, even the continuous portion of the lower latitude forerunners has essentially the same frequency distribution as the slope I waves that follow.

The most distinctive acoustic feature of subarctic (and arctic) waters is the absence of a deep sound channel (Johnson and Norris, 1968b). Although a shallow, subsurface, velocity minimum may exist in summer, propagation is predominantly RSR. Kutchale (1961) found that explosion signals which propagated through the Arctic Ocean exhibited a dispersion of frequencies which was nicely

explained by normal-mode theory. For a given mode, higher frequency energy is concentrated nearer the surface and propagates at a correspondingly lower group velocity.

Upon entering a region with warmer surface water, shallower ESR rays become sofar rays. This ducting of higher frequency energy into the sofar channel, which occurs over paths to the PMR hydrophones from the subarctic but not from the Mariana or southern Japan trenches, may therefore partially explain the spectral differences in abyssal T waves.

The appearance of a low-frequency cutoff on sonagrams of many subarctic abyssal T phases (Fig. 5) strongly suggests that their initial propagation is confined to a surface layer. According to Kibblewhite and Denham (1965), the minimum duct-depth L for trapping any modes for frequency f is

$$L = 0.54 c_0 (f^2 g)^{-1/3}$$

where c_0 is sound speed at the surface and g is a constant gradient of speed. Figure 6 is a graph of this equation for $c_0 = 1460 \text{ m sec}^{-1}$ and $g = 0.014 \text{ sec}^{-1}$. If 10 hz is taken as a typical low-cutoff frequency, it is seen that subarctic abyssal T waves are ducted within at least the upper 700 meters of water. The absence of lower frequencies must be ascribed to the absence of significant large-dimensioned scatterers at sufficient depth to excite antinodes for sound pressure for lower frequencies. At lower latitudes, scattering in much of this 700-meter layer, as from a rough thermocline, will occur within the sofar channel. Here the interference patterns of normal-mode propagation are not conditioned by a surface boundary and depths of antinodes are indeterminate. This may account for the lower frequencies of T-phase forerunners from the region of the Mariana and southern Japan trenches, although, alternatively, the abundance of seamounts over the paths from that region may be responsible.

The fact that slope I phases from the subarctic contain fre-

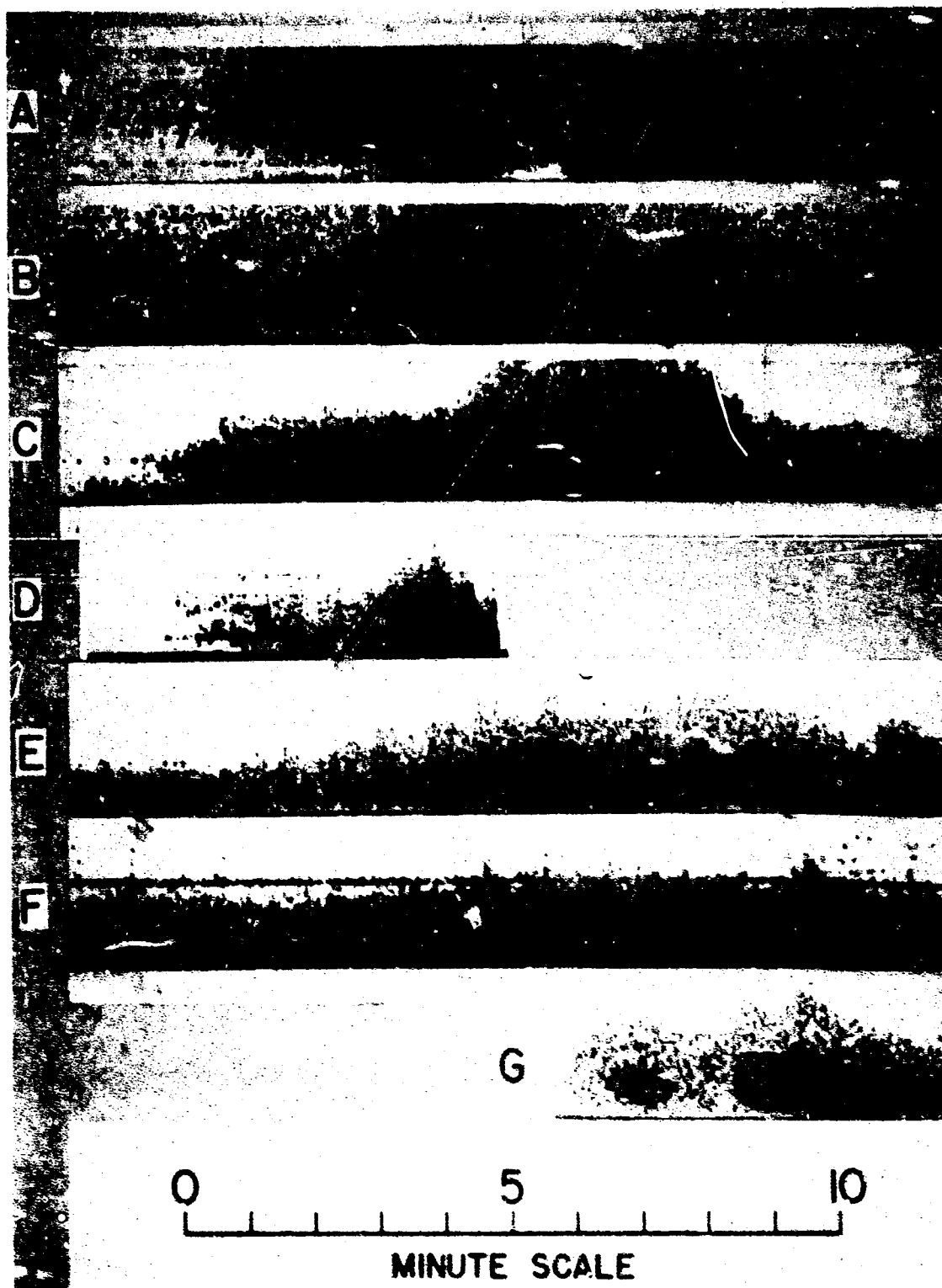


FIG. 1. 7 phases, with abnormal forerunners from the subarctic (A, B, and C) contrasted with those from lower latitudes. Source data are listed in Table IV.

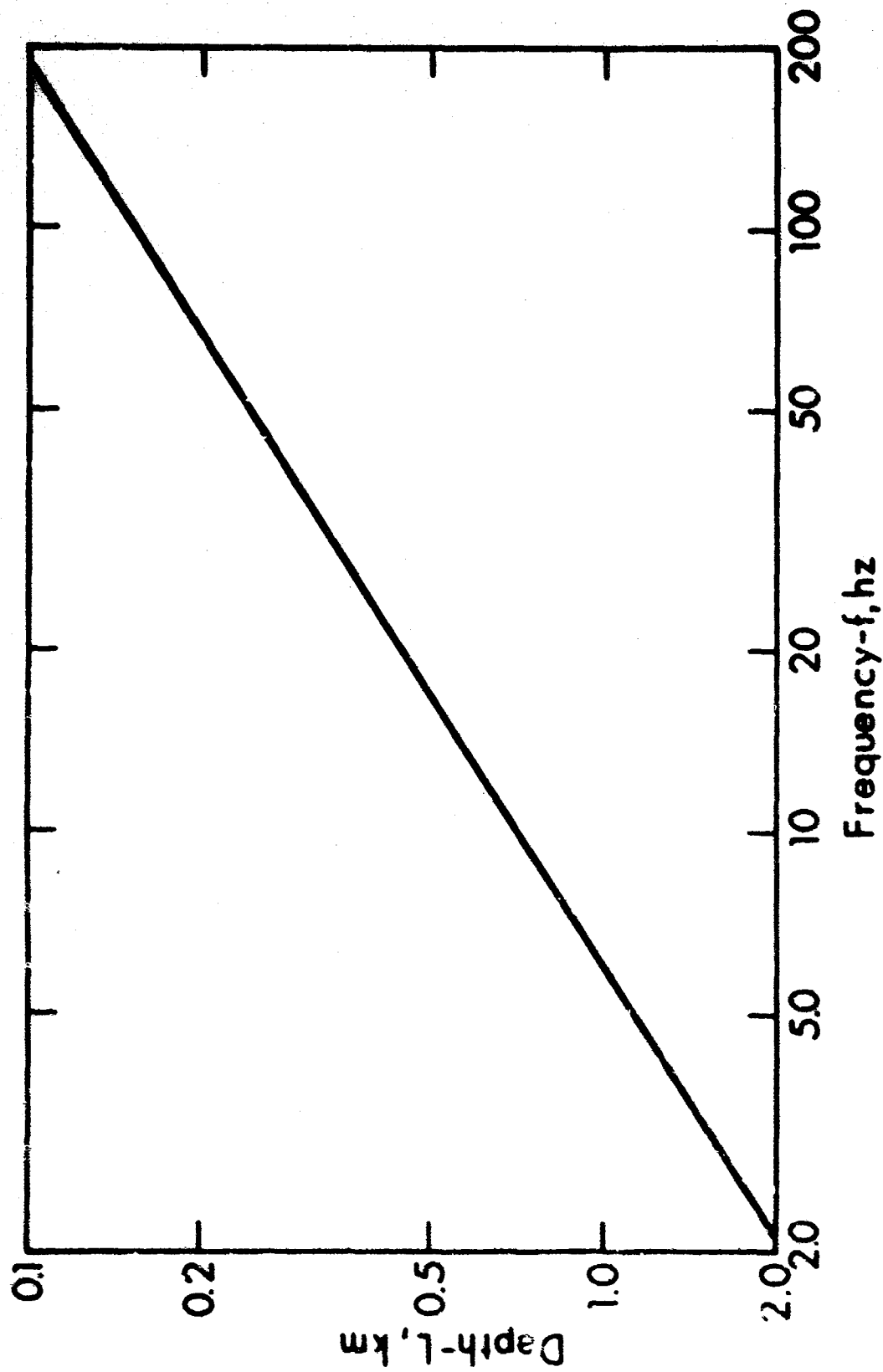


Fig. 6. Graph of the minimum depth of the RSR duct capable of trapping any mode at a given frequency. Sound speed at the surface is 1460 m sec^{-1} , with a constant gradient of 0.014 sec^{-1} .

quencies which are lower than those of their abyssally generated forerunners indicates excitation of RSR normal modes at greater depths. Nearly all of such energy will also be ducted into the sofar channel upon entering regions of warmer surface water.

CONCLUSION

Earthquakes under deep slopes generate T phases as efficiently as earthquakes under shallow slopes. In either case the short onset and decay rates indicate that the T waves are produced at radiators of restricted dimensions. In contrast, abyssal T phases, which are produced in the vicinity of trenches or over the flat ocean floor, show onset and decay rates for which a uniform scattering horizon is indicated. The production of T waves at a sloping bottom is ascribed to scattering from the bottom, either initially or in the course of multiple reflection within the water wedge.

Deep-slope T waves generated within the Central Pacific follow off-axis sofar paths. This hypothesis may be tested by comparing observed and predicted arrival times at Midway, with those at Wake, or at Eniwetok, from accurately located sources along the East Pacific Rise.

Abyssal T waves from the subarctic region are of distinctly higher frequencies than are abyssal T waves from lower latitudes. This difference is ascribed to downward ducting of higher frequency energy from the subarctic surface channel.

ACKNOWLEDGMENTS

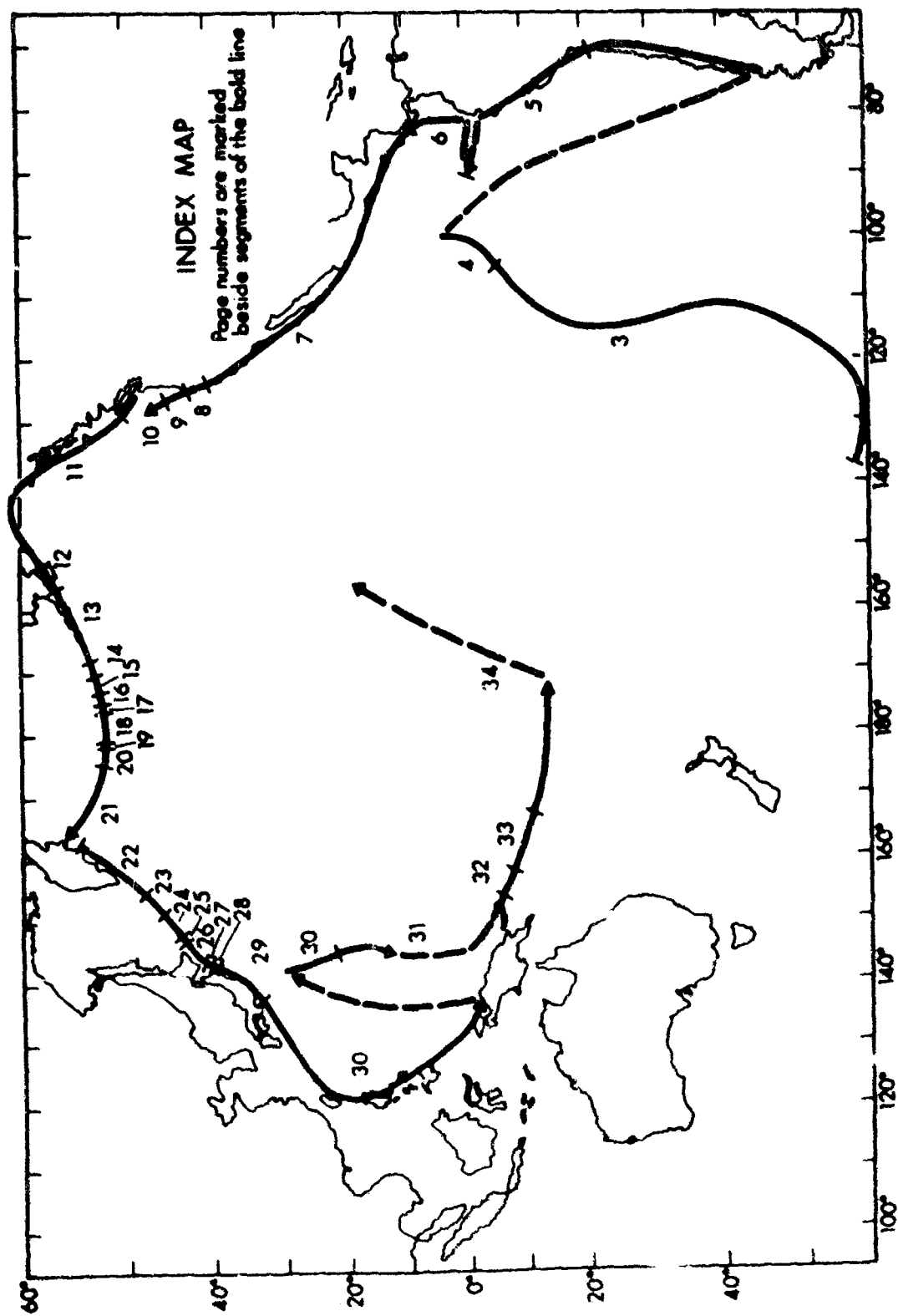
Hydrophone recording was conducted by the Pacific Missile Range. William M. Adams kindly allowed us the use of the sound spectrograph of the University of Hawaii Water Resources Research Center. This work was funded by the Advanced Research Projects Agency through Office of Naval Research contract Nonr 3748(01).

REFERENCES

- Atwater, Tanya M. and John D. Mudie, 1968: Block faulting on the Gorda Rise, *Science*, 159, pp. 729-731.
- Aubrat, J., 1963: Ondes T réfléchies dans la Mer des Antilles, *Ann. de Geophys.*, 19, pp. 386-405.
- Cooke, R. J. S., 1967: Observations of the seismic T phase at Macquarie Island, *N. Z. J. Geol. Geophys.*, 10, pp. 1212-1225.
- Duennebler, Frederick K., 1968: Spectral variation of the T phase, *Hawaii Institute of Geophysics Rept. HIG-68-22*, 18 pp.
- Duennebler, Frederick K. and Rockne H. Johnson, 1967: T-phase sources and earthquake epicenters in the Pacific Basin, *Hawaii Institute of Geophysics Rept. HIG-67-24*, 17 pp., with 83 pp. Appendix.
- Erickson, Barrett H., Frederic P. Naugler, and William H. Lucas, 1970: Emperor Fracture Zone: a newly discovered feature in the Central North Pacific, *Nature*, 225, pp. 53-54.
- Johnson, Rockne H., 1966: Routine location of T-phase sources in the Pacific, *Bull. Seism. Soc. Am.*, 56, pp. 109-118.
- Johnson, Rockne H. and Roger A. Norris, 1968a: T-phase radiators in the western Aleutians, *Bull. Seism. Soc. Am.*, 58, pp. 1-10.
- Johnson, Rockne H. and Roger A. Norris, 1968b: Geographic variation of sofar speed and axis depth in the Pacific Ocean, *J. Geophys. Res.*, 73, pp. 4695-4700.
- Johnson, Rockne H., Roger A. Norris, and Frederick K. Duennebler, 1968: Abyssally generated T phases, pp. 70-78 *In* Leon Knopoff, Charles L. Drake, and Pembroke J. Hart (eds.), *The Crust and Upper Mantle of the Pacific Area*, Am. Geophys. Union Geophys. Mono. No. 12.
- Johnson, Rockne H. and John Northrop, 1966: A comparison of earthquake magnitude with T-phase strength, *Bull. Seism. Soc. Am.*,

- 56, pp. 119-124.
- Johnson, Rockne H., John Northrop, and Robert Eppley, 1963:
Sources of Pacific T phases, *J. Geophys. Res.*, 68, pp. 4251-4260.
- Kibblewhite, A. C. and R. N. Denham, 1965: Experiment on propagation in surface sound channels, *J. Acoust. Soc. Am.*, 38, pp. 63-71.
- Kutchale, Henry, 1961: Long-range sound transmission in the Arctic Ocean, *J. Geophys. Res.*, 66, pp. 2189-2198.
- Menard, H. W., 1966: Fracture zones and offsets of the East Pacific Rise, *J. Geophys. Res.*, 71, pp. 682-685.
- Milne, A. K., 1959: Comparison of spectra of an earthquake T phase with similar signals from nuclear explosions, *Bull. Seism. Soc. Am.*, 49, pp. 317-327.
- Northrop, J., H. W. Menard, and F. K. Duennebie, 1968: Seismic and bathymetric evidence of a fracture zone on Gorda Ridge, *Science*, 161, pp. 688-690.
- Robertson, E. I. and A. C. Kibblewhite, 1966: Bathymetry around isolated islands and atolls in the South Pacific Ocean, *N. Z. J. Geol. Geophys.*, 9, pp. 111-121.
- Sykes, L. R., 1963: Seismicity of the South Pacific Ocean, *J. Geophys. Res.*, 68, pp. 5999-6006.
- Tolstoy, Ivan and Maurice Ewing, 1950: The T phase of shallow-focus earthquakes, *Bull. Seism. Soc. Am.*, 40, pp. 25-51.

APPENDIX



APPENDIX

The order of the sonagrams presented here is by geographic location starting on the East Pacific Rise and proceeding as diagrammed on the map on the facing page. Page numbers are written by segments of the position line.

The annotation of sonagrams, with few exceptions, is the annotation used on C&GS Preliminary Determination of Epicenters cards. Some events which were not located by C&GS but by hydrophone network are marked by a dagger and annotated in the form used in the HIG T-Phase Source Locations.

C&GS annotation:

29 DEC 66	22 16 22.7	32.8S	111.7N
EASTER ISLAND CORDILLERA		33R 5.4	24

area name

Greenwich time

depth,
km

magni-
tude

hydro-
phone no.

HIG T-Phase annotation:

†24 MAY 67	04 12 31	55.7S	136.6W
EAST PACIFIC RIDGE		7-4	44 23

area name

Greenwich time

number of
phones-no. of
stations

T-phase
strength,
db

hydro-
phone
no.

Hydrophones at Oahu, Midway, Wake, and Eniwetok are numbered in the 10's, 20's, 30's, and 40's, respectively.

The sonagrams display relative intensity contoured in the frequency-time plane. They have an intensity range of 42 db (seven 6 db contours). Frequencies range, vertically, from 0 to 50 hz. The duration of a single sonagram is 6.4 minutes.

09 DEC 64 11 22 22* 35.1S 109.7W
EASTER ISLAND CORDILLERA 33 47 44

18 NOV 66 09 12 09.9 36.3S 100.7W
SOUTHERN PACIFIC OCEAN 33R 51 24

01 NOV 67 19 38 16* 34.1S 112.4W
EASTER ISLAND CORDILLERA 33R 47 25

29 DEC 66 22 16 227 32.8S 111.7N
EASTER ISLAND CORDILLERA 33R 5.4 21

22 JAN 68 17 36 31* 28.5S 112.8W
EASTER ISLAND REGION 33R 4.6 24

29 JAN 68 09 16 31* 24.0S 115.7W
EASTER ISLAND CORDILLERA 33R 50 36

17 JUN 67 00 56 29.4 45.5S 104.7W
NORTH EASTER ISLAND CORDILLERA 33R 4.8 22

09 DEC 64 11 22 22* 35.1S 109.7W
EASTER ISLAND CORDILLERA 33 47 44

18 NOV 66 09 12 09.9 36.3S 100.7W
SOUTHERN PACIFIC OCEAN 33R 51 24

01 NOV 67 19 38 16* 34.1S 112.4W
EASTER ISLAND CORDILLERA 33R 47 25

29 DEC 66 22 16 227 32.8S 111.7N
EASTER ISLAND CORDILLERA 33R 5.4 21

22 JAN 68 17 36 31* 28.5S 112.8W
EASTER ISLAND REGION 33R 4.6 24

29 JAN 68 09 16 31* 24.0S 115.7W
EASTER ISLAND CORDILLERA 33R 50 36

17 JUN 67 00 56 29.4 45.5S 104.7W
NORTH EASTER ISLAND CORDILLERA 33R 4.8 22

18 DEC 67 18 29 07 3.6S 102.9W
OFF COCHILERA 33R 45 24

30 DEC 67 02 46 55 2.1N 101.1W
EAST CENTRAL PACIFIC 33R 47 23

28 MAR 68 12 44 38 2.6N 101.8W
EAST CENTRAL PACIFIC 33R 49 24

01 JAN 68 04 05 34 2.8N 101.1W
EAST CENTRAL PACIFIC 33R 45 24

01 APR 68 04 11 21 2.2N 84.3W
OFF CENTRAL AMERICA 33R 46 16

11 JAN 68 09 37 14 3.0N 84.3W
OFF CENTRAL AMERICA 48 48 24

19 JUN 68 19 58 09 43.9S 75.1W
SOUTH CHILE 24 57 32

26 SEP 67 11 11 23 33.6S 70.5W
CHILE-ARGENTINA BORDER 84 58 32

26 SEP 67 18 11 23 30.0S 71.3W
NEAR COAST OF CENTRAL CHILE 55R 6 32

27 MAR 67 22 15 02 22.7S 67.6W
CHILE-BOLIVIA BORDER 160 41 16

21 DEC 67 02 25 18 21.8S 70.0W
NORTH CHILE 33R 6.3 30

25 DEC 67 10 41 56 21.5S 70.4W
NORTH CHILE 53R 58 32

27 DEC 67 09 17 55 21.2S 68.3W
CHILE-BOLIVIA BORDER 135 64 37



08 NOV 67 10 47 453 200S 70.3W
NORTH CHILE 66 46 32



08 JAN 68 13 44 245 18.6S 69.9W
NORTH CHILE 116 54 43



21 DEC 67 07 50 348 16.4S 72.6W
PERU 99 50 32



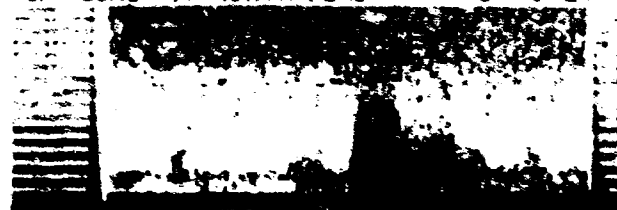
17 OCT 66 21 41 563 10.7S 78.7W
PERU 38 74 16



24 SEP 63 16 30 160 10.6S 78.0W
PERU 80 65 15



20 APR 67 14 07 233 8.3S 80.1W
OFF COAST OF NORTH PERU 78 46 24



19 JUN 68 13 44 314 0.9S 91.9W
GALAPAGOS ISLANDS 33R 46 16



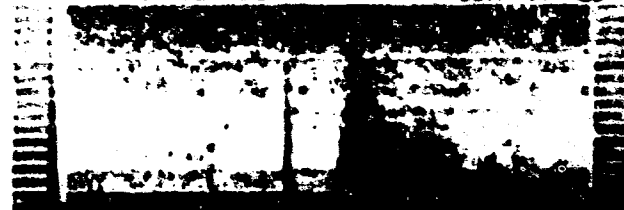
17 JUN 68 19 23 358 0.7S 91.7W
GALAPAGOS ISLANDS 33R 46 25



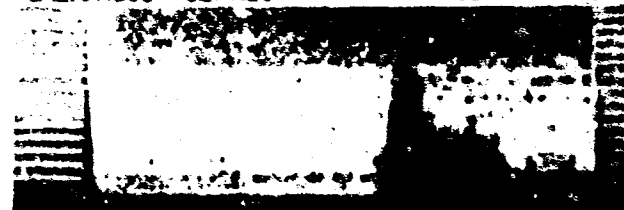
17 JUN 68 21 16 453 0.7S 91.7W
GALAPAGOS ISLANDS 33R 46 25



16 JUN 68 12 59 576 0.3S 91.7W
GALAPAGOS ISLANDS 33R 47 23



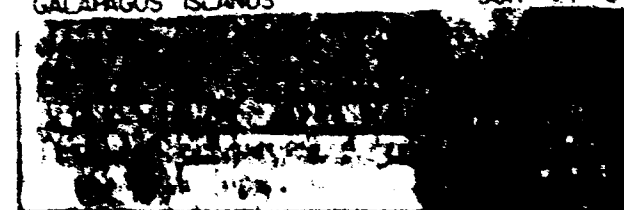
19 JUN 68 16 47 417 0.1S 91.7W
GALAPAGOS ISLANDS 33R 47 16



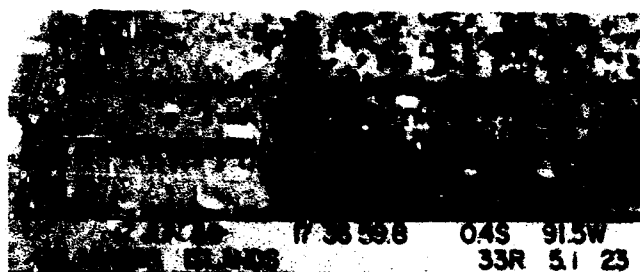
19 JUN 68 12 36 457 0.5S 91.6W
GALAPAGOS ISLANDS 33R 46 16



18 JUN 68 23 21 512 0.5S 91.5W
GALAPAGOS ISLANDS 33R 44 24



17 JUN 68 08 09 007 0.6S 91.5W
GALAPAGOS ISLANDS 33R 48 23



17 JUN 68 17 38 59.8 04S 91.5W
33R 51 23



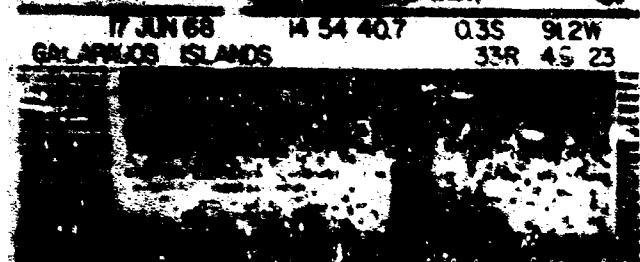
17 JUN 68 04 18 22.0 02S 91.5W
GALAPAGOS ISLANDS 33R 45 23



18 JUN 68 08 56 10.3 02S 91.5W
GALAPAGOS ISLANDS 33R 47 23



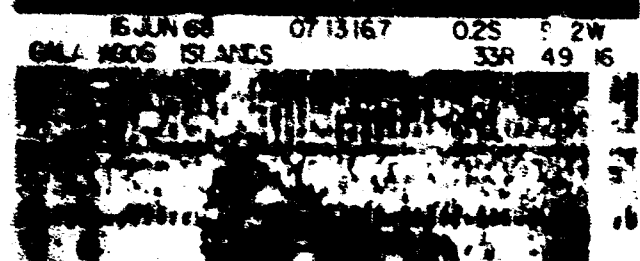
17 JUN 68 14 54 40.7 03S 91.2W
GALAPAGOS ISLANDS 33R 45 23



17 JUN 68 16 17 05.0 03S 91.2W
GALAPAGOS ISLANDS 33R 48 16



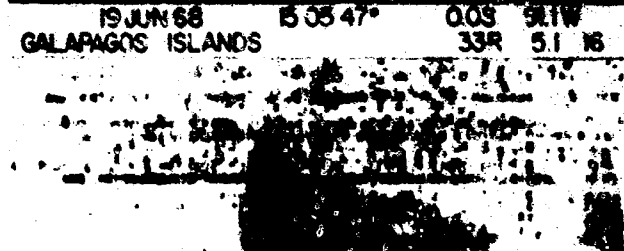
16 JUN 68 07 13 16.7 02S 91.2W
GALAPAGOS ISLANDS 33R 49 16



17 JUN 68 02 30 25.0 03S 91.2W
GALAPAGOS ISLANDS 33R 46 23



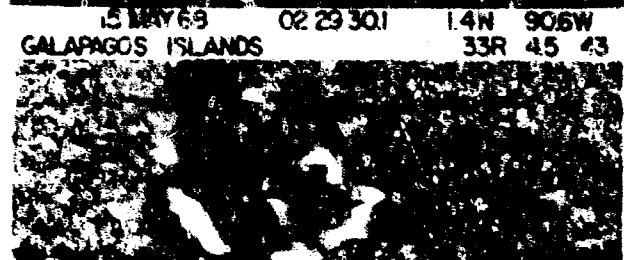
19 JUN 68 15 05 47.0 00S 91.1W
GALAPAGOS ISLANDS 33R 51 16



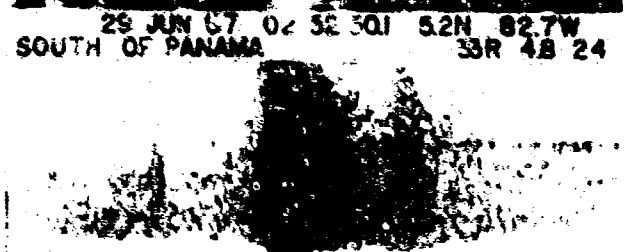
17 JUN 68 08 51 13.7 01N 91.3W
GALAPAGOS ISLANDS 33R 50 23



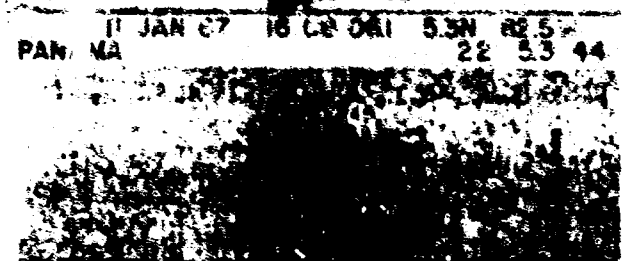
15 MAY 68 02 29 30.1 1.4N 90.6W
GALAPAGOS ISLANDS 33R 45 43



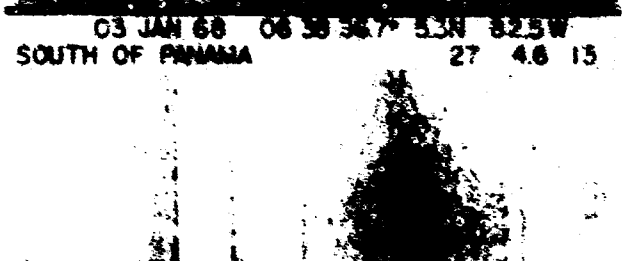
29 JUN 67 02 32 50.1 5.2N 82.7W
SOUTH OF PANAMA 33R 48 24



11 JAN 67 16 42 00.1 5.3N 82.5W
PANAMA 22 53 44



03 JAN 68 06 58 56.7 5.3N 82.5W
SOUTH OF PANAMA 27 46 13



23 APR 67 22 25 27.4 6.1N 81.3W
COSTA RICA 46 45 24

13 NOV 67 16 06 465 10.4N 85.7W
COSTA RICA 18 48 42

06 FEB 68 22 47 524 10.2N 103.7W
OFF MEXICO 53 48 24

20 JAN 68 21 41 098 16.1N 105.4W
MEXICO 51 48 16

03 JAN 68 19 14 566 10.9N 102.7W
OFF MEXICO 33R 46 13

30 JUN 68 20 04 341 17.9N 105.6W
MEXICO 33R 45 22

30 JUN 68 20 21 277 17.9N 105.8W
MEXICO 35 48 22

30 JUN 68 21 08 556 18.0N 105.5W
MEXICO 33R 40 22

04 APR 67 18 20 05 18.1N 105.1W
MEXICO

24 SEP 66 08 57 102 12.0N 130.8W
CENTRAL PACIFIC OCEAN 33 53 48

20 AUG 66 23 37 196 18.7N 107.0W
REVILLA GIGEDO 54 53 48

17 FEB 68 21 00 336 20.2N 108.1W
REVILLA GIGEDO 33R 41 16

23 APR 68 13 18 220 31.7N 116.9W
PINA CALIFORNIA 33R 47 16

18 DEC 67 17 24 319 37.0N 121.8W
CENTRAL CALIFORNIA COAST 11 5.0 23

27 JUN 68 11 22 456 40.0N 124.5W
NORTH CALIFORNIA 33R 42 13

26 JUN 68 04 19 20° 40.1N 124.5W
NORTH CALIFORNIA 33R 42 24

26 JUN 68 02 53 42° 40.1N 124.4W
NORTH CALIFORNIA 33R 41 34

26 JUN 68 02 29 09° 40.2N 124.7W
NORTH CALIFORNIA 33R 45 24

26 JUN 68 05 50 29.6 40.2N 124.6W
NORTH CALIFORNIA 33R 43 24

26 JUN 68 10 47 46.0 40.2N 124.4W
NORTH CALIFORNIA 33R 51 32

26 NOV 66 04 30 58° 40.3N 125.5W
OFF CALIFORNIA 33R 45 15

26 NOV 66 05 56 39° 40.3N 125.3W
OFF CALIFORNIA 33R 46 15

26 JUN 68 09 10 14.3 40.3N 124.6W
NORTH CALIFORNIA 33R 45 32

24 NOV 67 13 57 00.4 40.4N 125.1W
MENDOCINO ESCARPMENT (CALIFORNIA) 17 46 13

10 DEC 67 12 06 50.3 40.5N 124.6W
OFF NORTH CALIFORNIA 5 58 23

10 DEC 67 12 33 54.2 40.5N 125.0W
OFF NORTH CALIFORNIA 15 46 23

22 AUG 63 09 27 09.3 42.0N 126.2W
OFF OREGON 53 56 22

26 SEP 67 05 51 11° 42.0N 126.2W
OFF OREGON 33R 49 13

26 JUN 66 04 35 24° 42.2N 125.9W
OFF OREGON 33R 41 24

19 NOV 66 15 47 27° 42.2N 125.8W
OFF OREGON 33R 45 22

13 DEC 67 13 23 17° 42.6N 126.0W
OFF OREGON 33 4.4 24

13 DEC 67 10 12 44° 43.2N 125.9W
OFF OREGON 33R 4.3 24

31 AUG 65 11 26 23° 43.5N 126.0W
OFF OREGON 33 4.2 16

09 MAY 68 03 03 01.8 43.4N 127.0W
OFF OREGON 33R 5.2 43

13 NOV 67 17 44 13° 43.4N 126.8W
OFF OREGON 33 4.2 16

19 JAN 68 20 23 37.9 43.4N 126.6W
OFF OREGON 33 4.6 13

08 MAY 68 12 17 13.4 43.6N 127.1W
OFF OREGON 33R 4.8 13

19 FEB 68 18 03 10.4 43.6N 127.4W
OFF OREGON 33R 4.8 13

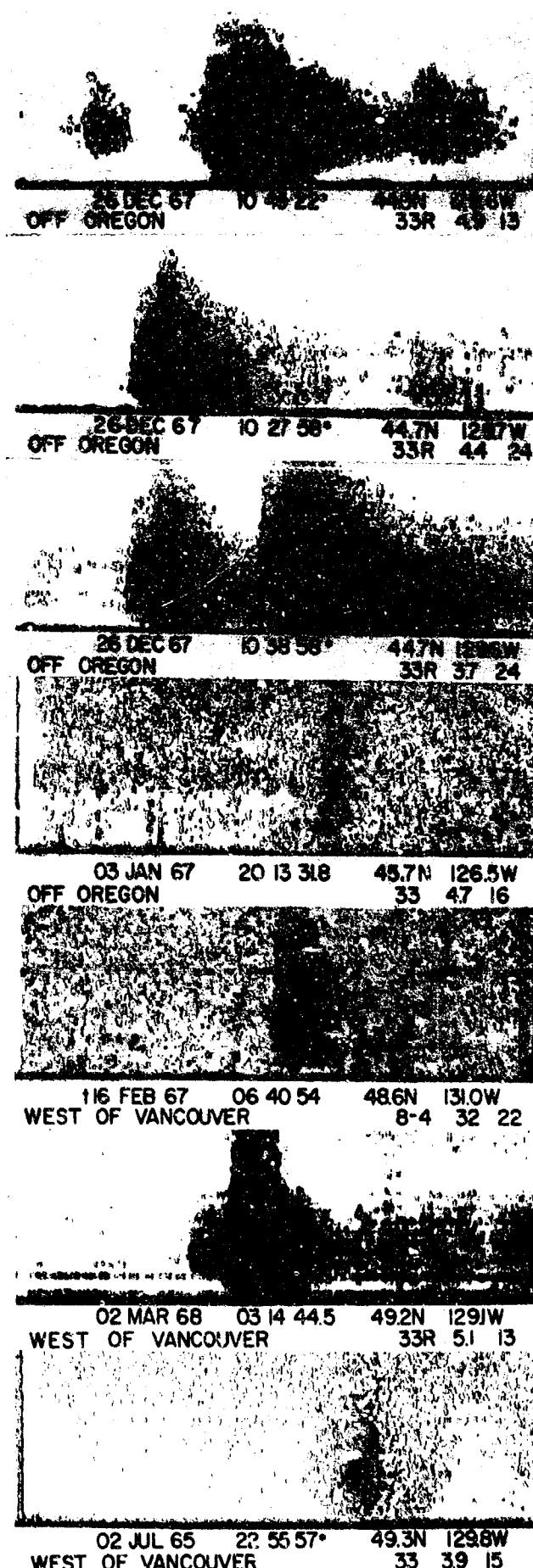
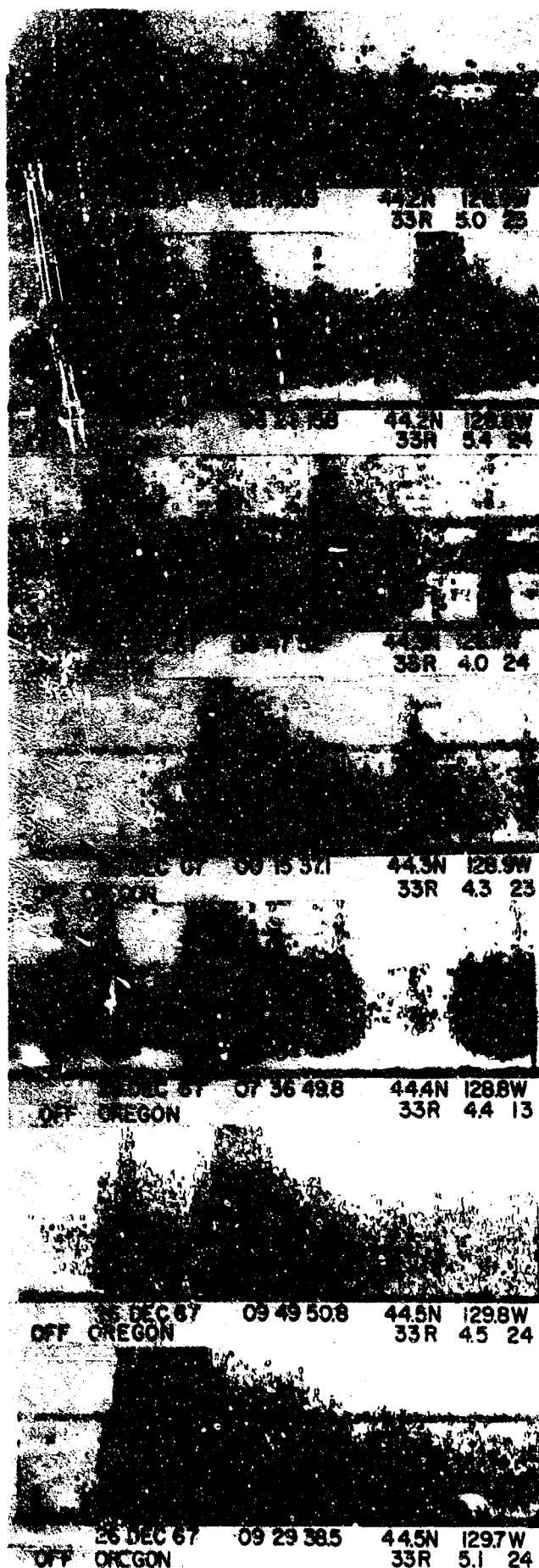
07 FEB 68 08 35 29.6 43.8N 127.5W
OFF OREGON 33R 5.1 24

09 JAN 68 11 44 52° 43.7N 127.6W
OFF OREGON 33R 4.4 10

04 DEC 67 08 48 45.2 43.7N 127.4W
OFF OREGON 33R 4.6 23

08 MAY 68 21 53 02.9 43.9N 128.2W
OFF OREGON 33R 4.6 44

28 DEC 67 07 01 36.8 44.2N 129.0W
OFF OREGON 33R 4.9 24



09 SEP 67 14 45 42* 498N 129.1W
WEST OF VANCOUVER 33R 4.0 13

123 MAR 67 11 57 51 50.0N 130.4W
QUEEN CHARLOTTE IS 11-4 8 16

01 FEB 68 07 58 03.5 50.0N 129.8W
WEST OF VANCOUVER 14 5.4 16

116 FEB 67 02 58 32 50.6N 130.6W
QUEEN CHARLOTTE IS 2 14-5 33

01 SEP 66 14 11 25* 50.6N 129.5W
WEST OF VANCOUVER 33 4.6 34

28 APR 67 00 00 41.8 51.2N 130.4W
QUEEN CHARLOTTE IS 6 5.1 24

30 MAR 64 07 09 340 59.9N 145.7W
GULF OF ALASKA 15 5.6 13

30 MAR 64 04 22 43.1 58.2N 146.3W
GULF OF ALASKA 15 4.6 13

30 MAR 64 01 32 09.5 59.8N 146.6W
GULF OF ALASKA 15 4.6 13

21 JUN 68 15 09 38.9 58.4N 148.1W
GULF OF ALASKA 33R 4.0 28

12 FEB 68 26 14 55.6 57.3N 149.8W
GULF OF ALASKA 33R 4.2 24

07 NOV 67 22 09 00.0 57.3N 150.0W
GULF OF ALASKA 33R 4.2 22

04 APR 68 06 07 54.5 56.3N 150.1W
GULF OF ALASKA 30 3.9 24

30 MAR 64 02 02 35* 56.7N 151.6W
KODIAK ISLAND REGION 33 4.2 13



30 MAR 64 05 32 30° 56.9N 151.7W
KODIAK ISLAND REGION 33 43 13



24 MAY 67 03 59 14° 56.7N 152.1W
KODIAK ISLAND REGION 14 40 16



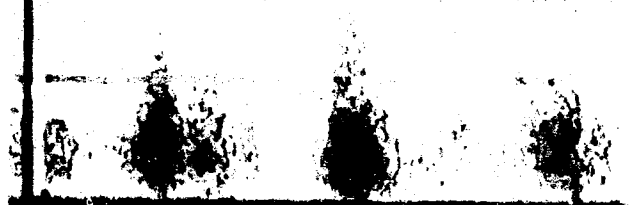
30 MAR 64 03 18 554 55.4N 152.6W
KODIAK ISLAND REGION 33 53 23



30 MAR 64 04 01 36° 56.4N 152.8W
KODIAK ISLAND REGION 33 43 13



30 MAR 64 02 18 063 56.6N 152.9W
KODIAK ISLAND REGION 25 58 13



30 MAR 64 02 41 596 56.5N 153.0W
KODIAK ISLAND REGION 30 49 13



30 MAR 64 08 40 107 56.5N 153.0W
KODIAK ISLAND REGION 20 43 13



30 MAR 64 08 53 179 56.2N 153.1W
KODIAK ISLAND REGION 30 43 13



29 MAR 64 23 08 266 56.1N 153.5W
KODIAK ISLAND REGION 15 46 23



30 MAR 64 03 12 171 56.0N 153.6W
KODIAK ISLAND REGION 33 41 13



10 APR 67 19 57 344 58.6N 154.3W
ALASKA PENINSULA 86 55 13



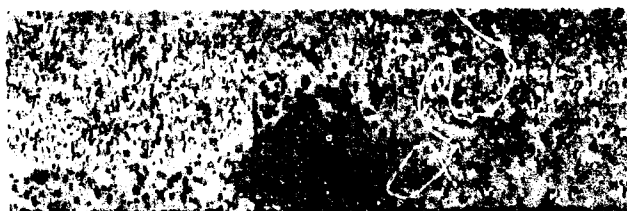
06 FEB 64 15 00 326 56.1N 154.3W
KODIAK ISLAND REGION 33 44 24



04 APR 67 09 00 083 55.5N 155.1W
SOUTH OF ALASKA 27 45 24



06 FEB 64 13 07 252 55.8N 155.8W
SOUTH OF ALASKA 33 56 32



07 FEB 67 14 53 13.9 56.7N 157.2W
ALASKA PENINSULA 67R 56 16



29 APR 66 01 46 43 53.8N 157.8W
SOUTH OF ALASKA 33 52 15



01 JUL 67 23 10 07.2 54.4N 158.0W
SOUTH OF ALASKA 33R 62 13



02 JUL 67 01 09 38.1 54.5N 158.1W
SOUTH OF ALASKA 33R 42 24



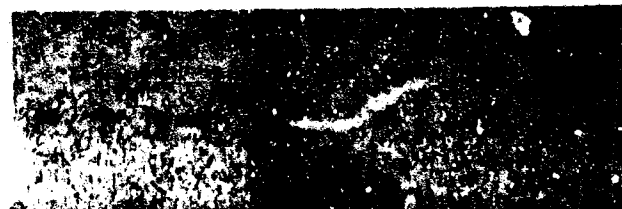
06 FEB 64 15 57 17 55.4N 160.8W
ALASKA PENINSULA 33 41 24



01 JUL 67 21 22 10.0 54.0N 161.0W
ALASKA PENINSULA 19 45 13



18 NOV 65 22 08 45.7 53.1N 161.8W
SOUTH OF ALASKA 8 53 44



16 SEP 66 17 10 39.0 53.8N 163.2W
UNIMAK ISLAND REGION 34 43 42



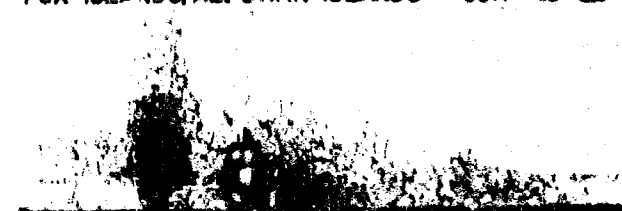
09 DEC 67 22 11 2.9 53.8N 163.2W
UNIMAK ISLAND REGION 14 43 42



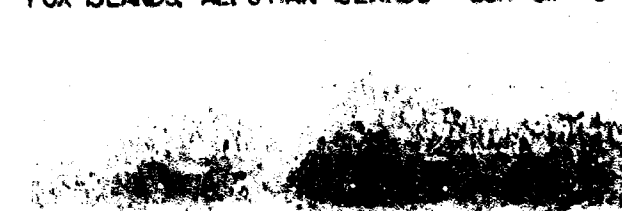
01 JUN 67 03 36 51 53.1N 163.2W
FOX ISLANDS, ALEUTIAN ISLANDS 60 57 23



19 OCT 67 01 22 20 52.7N 166.5W
FOX ISLANDS, ALEUTIAN ISLANDS 33R 43 22



19 JUN 67 17 01 45.4 52.7N 166.9W
FOX ISLANDS, ALEUTIAN ISLANDS 33R 57 13



02 SEP 66 21 13 19 53.7N 167.5W
FOX ISLANDS, ALEUTIAN ISLANDS 33 46 32



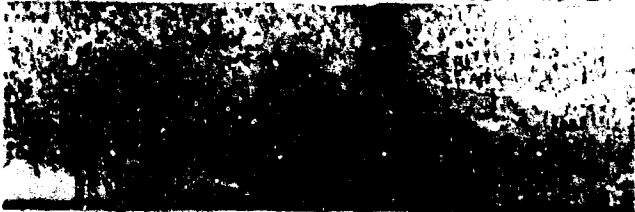
09 SEP 67 03 15 13 53.4N 167.5W
FOX ISLANDS, ALEUTIAN ISLANDS 33R 41 22



02 JUL 65 20 58 40S 53.1N 1676W
FOX ISLANDS, ALEUTIAN ISLANDS 60 67 28



27 DEC 67 05 34 52° 52.9N 168.0W
FOX ISLANDS, ALEUTIAN ISLANDS 33R 4.5 24



16 JAN 67 08 16 22.0 52.5N 168.3W
FOX ISLANDS, ALEUTIAN ISLANDS 37 57 13



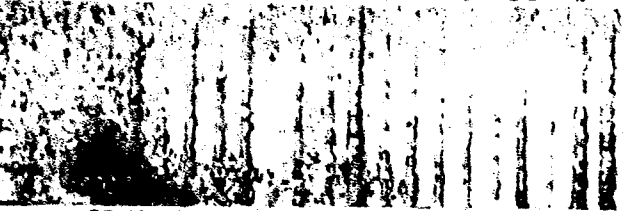
18 JAN 67 09 05 59° 52.4N 168.3W
FOX ISLANDS, ALEUTIAN ISLANDS 33 3.8 13



30 MAY 67 10 00 23 51.8N 168.6W
FOX ISLANDS, ALEUTIAN ISLANDS 33 4.2 16



28 JAN 67 16 00 09° 52.9N 169.3W
FOX ISLANDS, ALEUTIAN ISLANDS 33 3.5 16



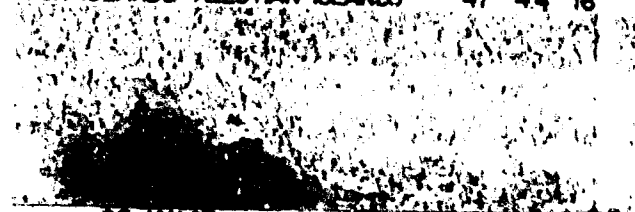
28 JAN 67 16 31 21 52.5N 169.3W
FOX ISLANDS, ALEUTIAN ISLANDS 32 5.6 16



28 JAN 67 15 34 21° 52.5N 169.4W
FOX ISLANDS, ALEUTIAN ISLANDS 33 4.6 16



28 JAN 67 20 49 34.0 52.5N 169.4W
FOX ISLANDS, ALEUTIAN ISLANDS 47 4.4 16



28 JAN 67 17 42 01.5 52.4N 169.4W
FOX ISLANDS, ALEUTIAN ISLANDS 50R 5.6 16



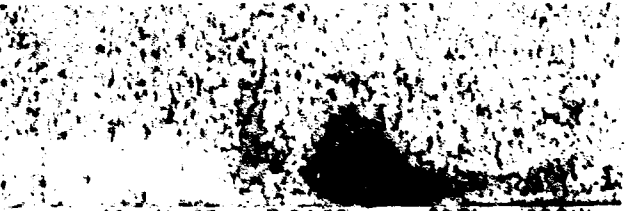
28 JAN 67 18 53 31° 52.4N 169.4W
FOX ISLANDS, ALEUTIAN ISLANDS 54 4.2 16



28 JAN 67 17 26 32.8 52.3N 169.4W
FOX ISLANDS, ALEUTIAN ISLANDS 33 4.3 16



28 JAN 67 20 10 21° 52.0N 169.4W
FOX ISLANDS, ALEUTIAN ISLANDS 33 4.2 16



28 JAN 67 17 04 58 52.7N 169.9W
FOX ISLANDS, ALEUTIAN ISLANDS 11-5 12 16



28 JAN 67 21 02 55° 52.5N 169.5W
FOX ISLANDS, ALEUTIAN ISLANDS 33 3.8 16



25 JAN 68 11 22 22.0 51.5N 169.6W
FOX ISLANDS, ALEUTIAN ISLANDS 33 4.7 16



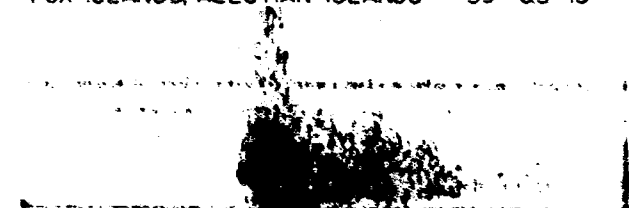
28 JAN 67 15 45 22° 52.2N 169.6W
FOX ISLANDS, ALEUTIAN ISLANDS 33 4.0 16



04 JAN 68 00 57 44.4 52.2N 171.3W
FOX ISLANDS, ALEUTIAN ISLANDS 36 5.7 23



07 AUG 66 02 13 05.1 50.6N 171.3W
FOX ISLANDS, ALEUTIAN ISLANDS - 39 6.5 15



11 AUG 67 10 43 30 52.3N 171.4W
FOX ISLANDS, ALEUTIAN ISLANDS 38 4.3 23



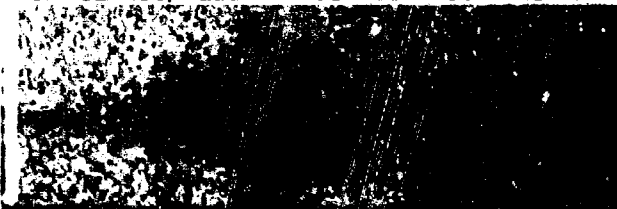
29 JUL 65 08 29 21.2 50.9N 171.4W
FOX ISLANDS, ALEUTIAN ISLANDS 22 6.3 15



29 JUL 65 11 13 38° 51.4N 171.5W
FOX ISLANDS, ALEUTIAN ISLANDS 33 4.0 30



29 JUL 65 09 32 00.8 51.1N 171.7W
FOX ISLANDS, ALEUTIAN ISLANDS 33 4.5 44



22 SEP 65 07 27 33.8 50.6N 172.8W
ANDREANOF ISLANDS, ALEUTIAN IS 36 4.6 15



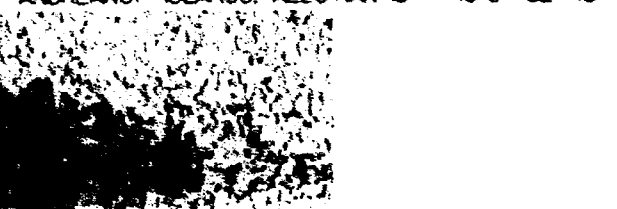
11 MAY 67 03 16 56 52.2N 173.4W
ANDREANOF ISLANDS, ALEUTIAN IS 13-5 23 13



11 MAY 67 03 20 12 52.2N 173.4W
ANDREANOF ISLANDS, ALEUTIAN IS 15-5 32 13



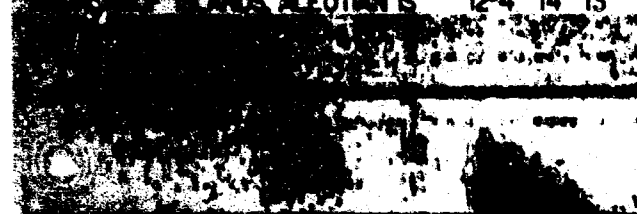
11 MAY 67 03 20 12 52.2N 173.4W
ANDREANOF ISLANDS, ALEUTIAN IS 15-5 32 13



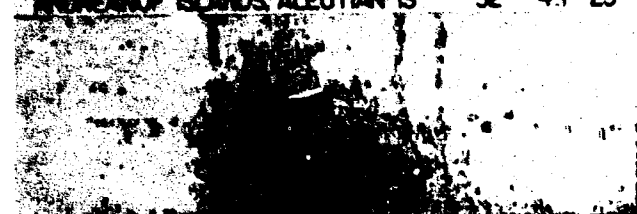
11 MAY 67 03 20 12 52.2N 173.4W
ANDREANOF ISLANDS, ALEUTIAN IS 15-5 32 13



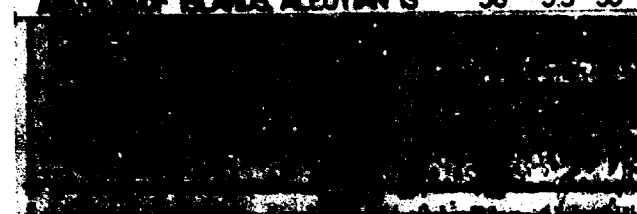
03 03 44 52.1N 173.4W
ANDREANOF ISLANDS, ALEUTIAN IS 12-4 14 13



05 MAY 68 11 12 002 51.7N 173.4W
ANDREANOF ISLANDS, ALEUTIAN IS 32 4.1 23



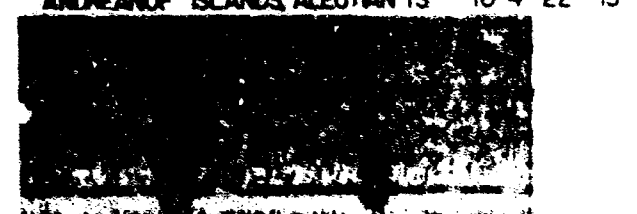
05 DEC 67 09 05 13.1 51.6N 173.4W
ANDREANOF ISLANDS, ALEUTIAN IS 36 5.3 30



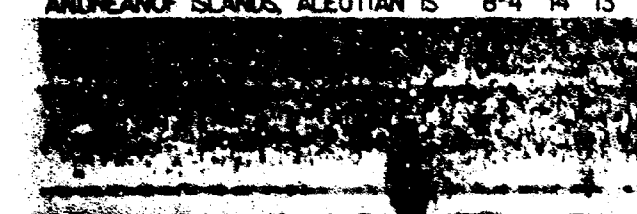
13 MAY 67 07 53 12 52.2N 173.5W
ANDREANOF ISLANDS, ALEUTIAN IS 10-4 26 13



13 MAY 67 07 14 06 51.9N 173.5W
ANDREANOF ISLANDS, ALEUTIAN IS 10-4 22 13



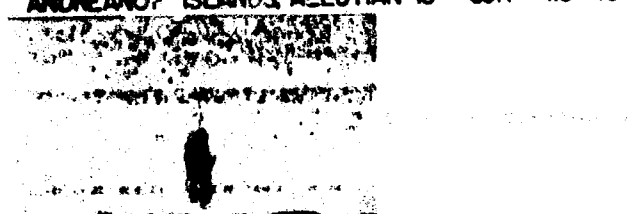
13 MAY 67 07 16 26 51.9N 173.5W
ANDREANOF ISLANDS, ALEUTIAN IS 8-4 14 13



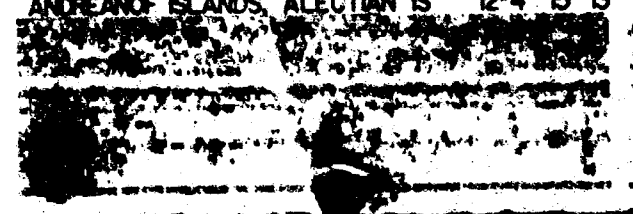
13 MAY 67 07 04 05 51.8N 173.5W
ANDREANOF ISLANDS, ALEUTIAN IS 12-4 30 13



09 DEC 67 23 53 53 51.8N 173.5W
ANDREANOF ISLANDS, ALEUTIAN IS 33R 4.0 43



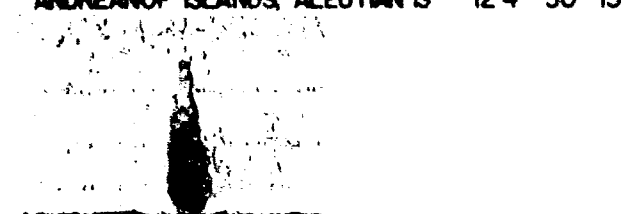
13 MAY 67 03 14 44 50.0N 173.5W
ANDREANOF ISLANDS, ALEUTIAN IS 12-4 15 13



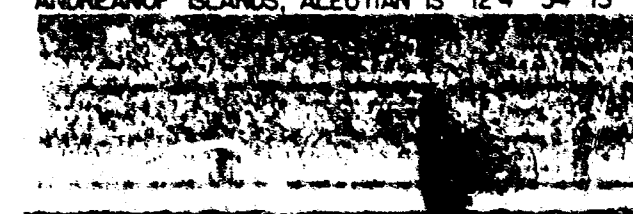
13 MAY 67 06 18 11 52.3N 173.6W
ANDREANOF ISLANDS, ALEUTIAN IS 35R 4.3 13



13 MAY 67 06 42 55 52.0N 173.6W
ANDREANOF ISLANDS, ALEUTIAN IS 12-4 30 13



13 MAY 67 06 39 20 51.8N 173.6W
ANDREANOF ISLANDS, ALEUTIAN IS 12-4 34 13



13 MAY 67 06 58 09 51.6N 173.6W
ANDREANOF ISLANDS, ALEUTIAN IS 2-4 31 13



13 MAY 67 01 08 39 52.2N 174.8W
ANDREANOF ISLANDS, ALEUTIAN IS 58 40 23

21 FEB 68 06 18 21.6 52.3N 175.3W
ANDREANOF ISLANDS, ALEUTIAN IS 108 5.2 16

22 FEB 68 12 53 33* 51.5N 175.6W
ANDREANOF ISLANDS, ALEUTIAN IS 20 4.3 24

21 FEB 68 19 32 32.2 51.7N 175.9W
ANDREANOF ISLANDS, ALEUTIAN IS 54 4.8 23

21 FEB 68 21 28 17* 51.7N 176.0W
ANDREANOF ISLANDS, ALEUTIAN IS 49 4.2 23

07 DEC 66 22 09 02* 51.7N 176.0W
ANDREANOF ISLANDS, ALEUTIAN IS 64 4.7 16

21 FEB 68 19 30 04.9 51.6N 176.0W
ANDREANOF ISLANDS, ALEUTIAN IS 57 4.7 23

25 FEB 68 18 08 19.9 51.4N 176.0W
ANDREANOF ISLANDS, ALEUTIAN IS 50 5.3 13

21 FEB 68 21 07 56.9 51.4N 176.0W
ANDREANOF ISLANDS, ALEUTIAN IS 47 5.2 24

22 FEB 68 16 49 58.6 51.4N 176.1W
ANDREANOF ISLANDS, ALEUTIAN IS 54 4.5 23

21 FEB 68 19 08 39.3 51.4N 176.1W
ANDREANOF ISLANDS, ALEUTIAN IS 49 4.7 23

22 FEB 68 14 43 46* 51.6N 176.2W
ANDREANOF ISLANDS, ALEUTIAN IS 65 3.8 23

22 FEB 68 17 46 57.4 51.4N 176.2W
ANDREANOF ISLANDS, ALEUTIAN IS 49 5.1 23

22 FEB 68 17 56 40* 51.4N 176.2W
ANDREANOF ISLANDS, ALEUTIAN IS 56 4.1 23

22 FEB 68 13 13 59.3 51.4N 176.2W
ANDREANOF ISLANDS, ALEUTIAN IS 66 4.4 23

23 FEB 68 0010 39.5 51.5N 176.3W
ANDREANOF ISLANDS, ALEUTIAN IS 65 4.5 13

15 NOV 66 16 26 05 51.5N 176.5W
ANDREANOF ISLANDS, ALEUTIAN IS 61 4.5 23

30 MAY 67 09 54 38.3 50.1N 176.6W
ANDREANOF ISLANDS, ALEUTIAN IS 30R 50 23

01 OCT 65 09 14 29 51.5N 176.3W
ANDREANOF ISLANDS, ALEUTIAN IS 33 4.1 15

29 APR 67 03 55 20.8 51.4N 178.3W
ANDREANOF ISLANDS, ALEUTIAN IS 50 6.0 44

07 SEP 66 05 28 44.2 51.2N 179.2W
ANDREANOF ISLANDS, ALEUTIAN IS 33 4.8 24

14 MAY 69 19 32 54.2 51.3N 179.9W
ANDREANOF ISLANDS, ALEUTIAN IS 21 6.2 42

29 JUN 67 04 53 25.0 51.7N 177.0W
ANDREANOF ISLANDS, ALEUTIAN IS 58 4.6 23

28 JAN 66 19 07 15.0 51.7N 177.0W
ANDREANOF ISLANDS, ALEUTIAN IS 54 5.2 15

23 FEB 66 01 40 12 51.6N 177.2W
ANDREANOF ISLANDS, ALEUTIAN IS 54 4.5 13

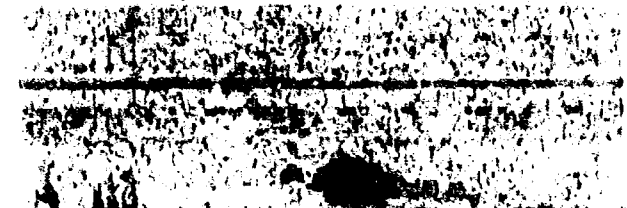
29 JAN 68 11 49 18.7 51.2N 179.1E
RAT ISLANDS, ALEUTIAN ISLANDS 45 4.6 13

08 NOV 67 17 03 04.1 51.1N 178.7E
RAT ISLANDS, ALEUTIAN ISLANDS 42 5.3 13

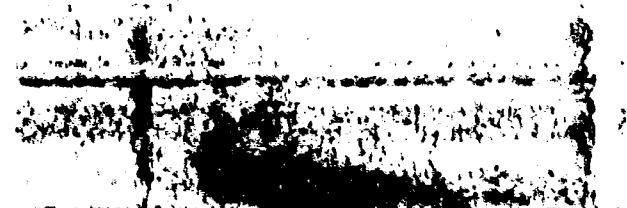
08 NOV 67 17 09 27.1 51.1N 178.7E
RAT ISLANDS, ALEUTIAN ISLANDS 29 5.3 13



08 NOV 67 17 22 32.1 51.1N 178.7E
RAT ISLANDS, ALEUTIAN ISLANDS 10 53 13



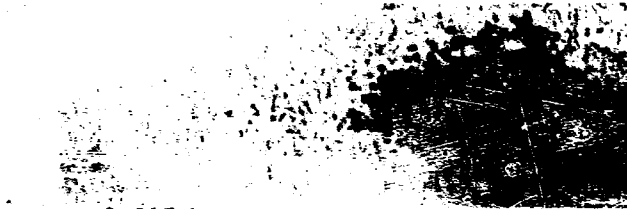
08 NOV 67 19 40 27.0 51.1N 178.7E
RAT ISLANDS, ALEUTIAN ISLANDS 42 53 24



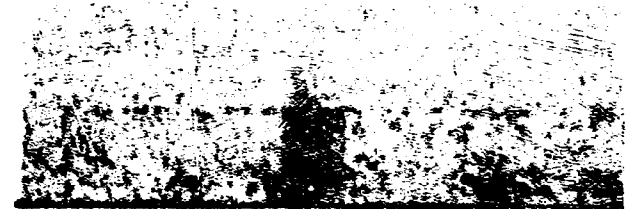
08 NOV 67 19 53 55.5 51.1N 178.4E
RAT ISLANDS, ALEUTIAN ISLANDS 32 46 24



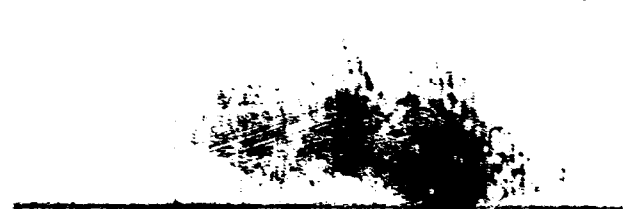
30 MAR 65 08 54 18.0 50.1N 178.3E
RAT ISLANDS, ALEUTIAN ISLANDS 33 43 16



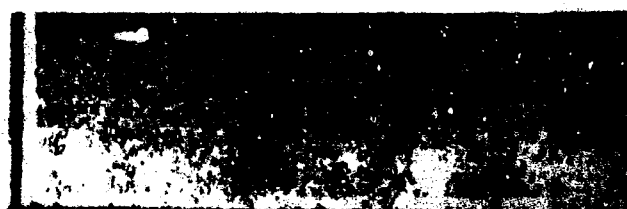
01 OCT 65 08 52 04.4 50.1N 178.2E
RAT ISLANDS, ALEUTIAN ISLANDS 23 63 24



01 OCT 65 09 09 41.0 50.1N 178.2E
RAT ISLANDS, ALEUTIAN ISLANDS 16 51 24



11 MAR 68 18 25 13.3 52.1N 178.2E
RAT ISLANDS, ALEUTIAN ISLANDS 121 52 32



30 MAR 65 09 05 12.7 50.2N 177.9E
RAT ISLANDS, ALEUTIAN ISLANDS 38 47 16



30 MAR 65 03 02 57.0 50.4N 177.9E
RAT ISLANDS, ALEUTIAN ISLANDS 30 51 16



30 MAR 65 02 27 07.2 50.6N 177.9E
RAT ISLANDS, ALEUTIAN ISLANDS 51 7 28



29 JUL 65 07 08 19.0 51.4N 177.9E
RAT ISLANDS, ALEUTIAN ISLANDS 33 49 24



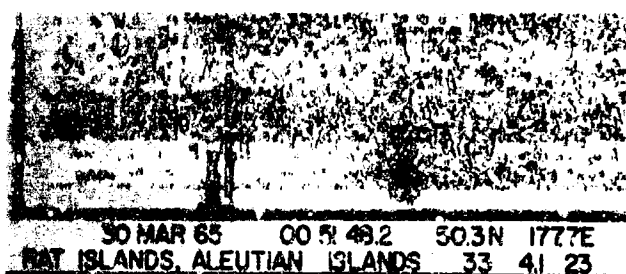
30 MAR 65 07 10 53.4 50.2N 177.8E
RAT ISLANDS, ALEUTIAN ISLANDS 35 49 16



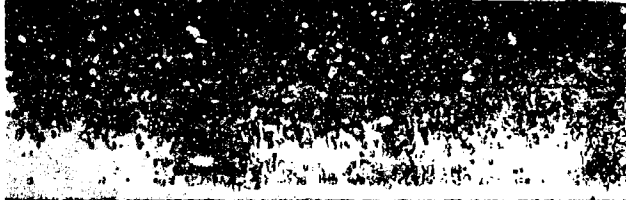
30 MAR 65 07 10 53.4 50.2N 177.8E
RAT ISLANDS, ALEUTIAN ISLANDS 35 49 16



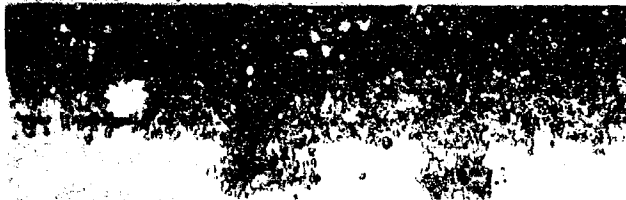
30 MAR 65 07 21 06.0 50.2N 177.7E
RAT ISLANDS, ALEUTIAN ISLANDS 33 50 16



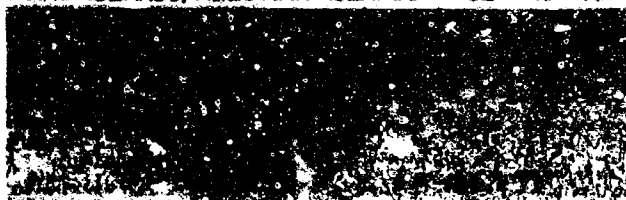
30 MAR 65 00 51 49.2 50.3N 177.7E
RAT ISLANDS, ALEUTIAN ISLANDS 33 41 23



30 MAR 65 08 11 07.3 50.5N 177.5E
RAT ISLANDS, ALEUTIAN ISLANDS 35 47 16



30 MAR 65 07 40 37.5 50.3N 177.4E
RAT ISLANDS, ALEUTIAN ISLANDS 32 47 16



30 MAR 65 06 25 01.1 50.1N 177.3E
RAT ISLANDS, ALEUTIAN ISLANDS 30 52 16



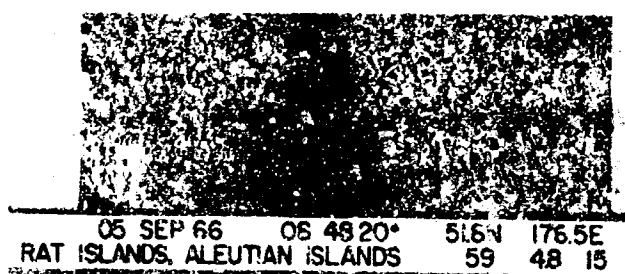
15 AUG 65 20 51 06* 51.5N 177.0E
RAT ISLANDS, ALEUTIAN ISLANDS 33 41 22



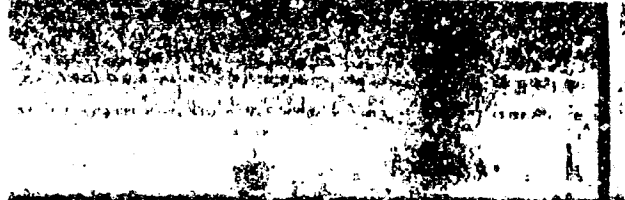
26 DEC 67 14 41 27* 51.7N 176.9E
RAT ISLANDS, ALEUTIAN ISLANDS 33R 43 23



30 MAR 65 08 29 48* 51.7N 176.9E
RAT ISLANDS, ALEUTIAN ISLANDS 33 37 16



05 SEP 66 08 48 20* 51.6N 176.5E
RAT ISLANDS, ALEUTIAN ISLANDS 59 48 15



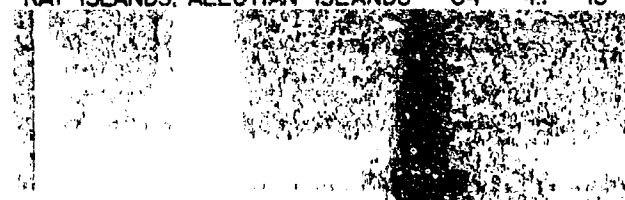
30 MAR 65 09 53 00.6 50.5N 176.0E
RAT ISLANDS, ALEUTIAN ISLANDS 33 48 16



129 MAY 67 03 41 05 51.7N 175.9E
RAT ISLANDS, ALEUTIAN ISLANDS 11-4 24 23



04 NOV 65 10 18 42* 52.0N 175.7E
RAT ISLANDS, ALEUTIAN ISLANDS 64 41 15



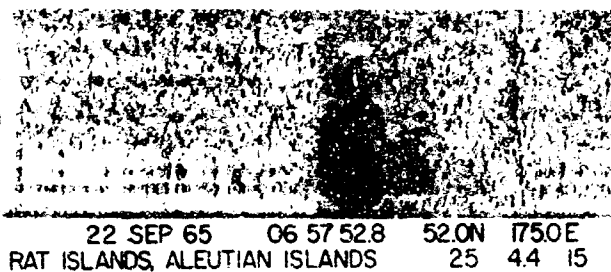
31 AUG 65 09 46 01* 51.5N 175.5E
RAT ISLANDS, ALEUTIAN ISLANDS 33 37 16



02 JUL 65 20 19 41.7 52.1N 175.4E
RAT ISLANDS, ALEUTIAN ISLANDS 37 54 15



06 AUG 66 21 04 32.5 51.9N 175.3E
RAT ISLANDS, ALEUTIAN ISLANDS 30 53 16



22 SEP 65 06 57 52.8 52.0N 175.0E
RAT ISLANDS, ALEUTIAN ISLANDS 25 44 15



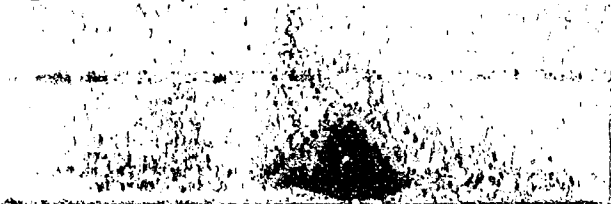
17 AUG 66 20 58 35.9 52.3N 174.9E
NEAR ISLANDS, ALEUTIAN ISLANDS 32 56 22



26 FEB 68 10 39 06.2 51.1N 174.6E
NEAR ISLANDS, ALEUTIAN ISLANDS 33R 47 30



23 MAR 67 08 45 20.2 52.3N 174.0E
NEAR ISLANDS, ALEUTIAN ISLANDS 62 44 16



07 MAY 67 11 03 49.5 51.8N 173.8E
NEAR ISLANDS, ALEUTIAN ISLANDS 18 46 24



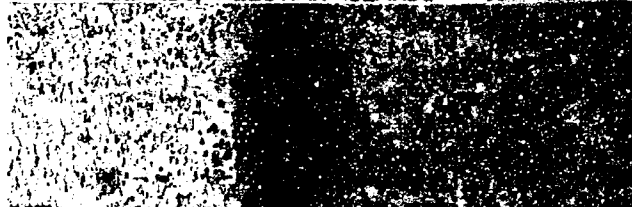
31 OCT 66 05 43 31* 52.1N 173.1E
NEAR ISLANDS, ALEUTIAN ISLANDS 33R 43 34



26 FEB 68 09 28 54.1 52.7N 172.6E
NEAR ISLANDS, ALEUTIAN ISLANDS 56 50 30



31 AUG 65 11 59 22* 52.3N 174.9E
NEAR ISLANDS, ALEUTIAN ISLANDS 33 51 44



28 APR 68 04 18 15.7 44.8N 174.4E
NORTH PACIFIC OCEAN 39 55 23



28 APR 68 06 23 02* 44.8N 174.7E
NORTH PACIFIC OCEAN 33R 43 23



16 OCT 65 20 01 52.9 56.1N 164.6E
KOMANDORSKY 41 54 30



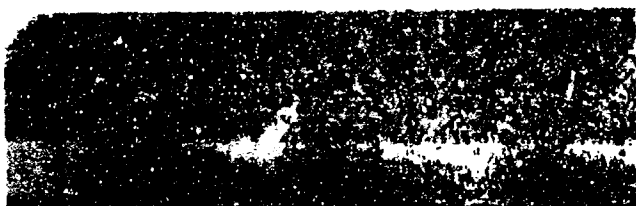
23 JAN 67 21 45 33* 55.3N 163.0E
NEAR EAST COAST OF KAMCHATKA 33R 43 35



23 DEC 66 23 49 27* 54.8N 162.5E
NEAR EAST COAST OF KAMCHATKA 28 49 16



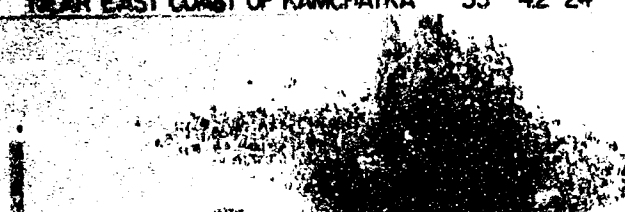
06 JUL 65 04 58 55.6 55.0N 162.0E
NEAR EAST COAST OF KAMCHATKA 34 52 22



23 DEC 66 23 56 09° 54.5N 162.2E
NEAR EAST COAST OF KAMCHATKA 33 4.6 16



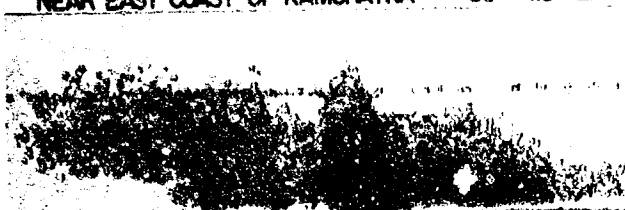
06 JUL 65 06 12 41° 54.3N 160.1E
NEAR EAST COAST OF KAMCHATKA 33 4.2 24



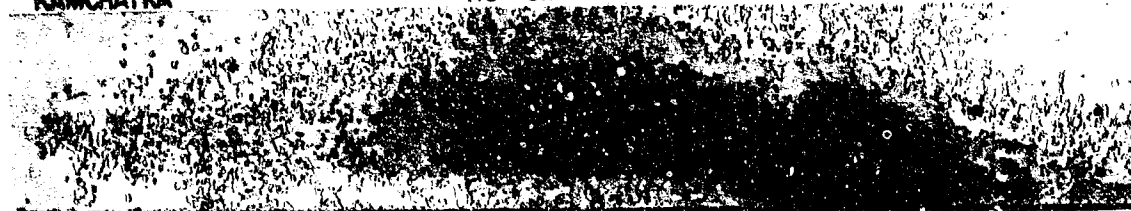
18 NOV 65 21 58 19.6 53.9N 160.6E
NEAR EAST COAST OF KAMCHATKA 67 0.1 44



01 JUL 65 11 51 56° 53.8N 160.4E
NEAR EAST COAST OF KAMCHATKA 65 4.3 22



18 JAN 67 22 28 01.2 55.0N 160.2E
KAMCHATKA 113 5.1 22



28 JAN 66 22 38 13.7 51.6N 157.0E
NEAR EAST COAST OF KAMCHATKA 112 5.7 22



12 MAR 67 01 23 49.5 51.1N 157.9E
NEAR EAST COAST OF KAMCHATKA 21 5.2 34



06 DEC 66 07 18 40° 50.1N 159.8E
KURIL ISLANDS 27 5.4 24



24 MAY 67 01 35 57° 50.0N 159.3E
KURIL ISLANDS 43 4.4 24



13 DEC 67 10 58 21.6 49.4N 154.6E
KURIL ISLANDS 138 5.1 24




18 JAN 66 04 20 52.9 48.9N 154.9E
KURIL ISLANDS 40 5.4 13



22 SEP 65 07 55 21° 48.7N 155.1E
KURIL ISLANDS 33 4.5 34




01 NOV 67 16 30 57.1 48.3N 154.4E
KURIL ISLANDS 40 5.5 44




01 NOV 67 16 09 16.7 48.2N 154.4E
KURIL ISLANDS 47 5.3 44




02 MAY 68 02 55 41* 48.2N 154.0E
KURIL ISLANDS 48 4.3 34




26 SEP 67 06 47 11.6 48.9N 150.6E
KURIL ISLANDS 136 4.7 22




06 FEB 64 09 40 16* 47.8N 152.4E
KURIL ISLANDS 65 4.3 32



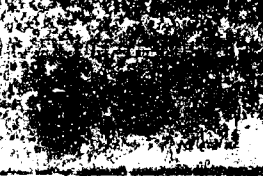
06 JUL 65 04 08 47.4 46.8N 152.5E
KURIL ISLANDS 39 5.6 22




13 DEC 67 10 38 23.4 47.6N 152.6E
KURIL ISLANDS 124 5.5 24



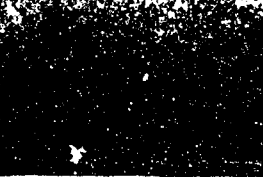
14 AUG 65 01 27 18.0 47.3N 153.1E
KURIL ISLANDS 41 4.4 24




22 APR 67 23 00 32 46.8N 151.6E
KURIL ISLANDS 73 4.4 16




26 SEP 67 06 47 11.6 46.9N 150.6E
KURIL ISLANDS 136 4.7 13




07 DEC 66 17 17 42.0 44.3N 151.7E
KURIL ISLANDS 26 5.8 32



16 MAY 67 05 08 31.6 45.5N 149.8E
KURIL ISLANDS 52R 4.7 16



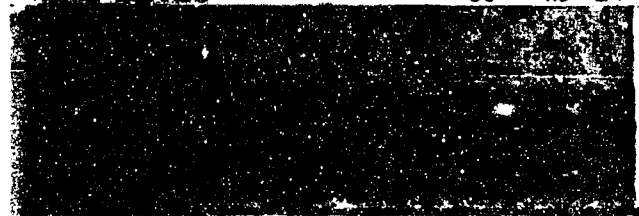
10 NOV 67 20 48 25.7 45.3N 149.8E
KURIL ISLANDS 95R 4.8 44



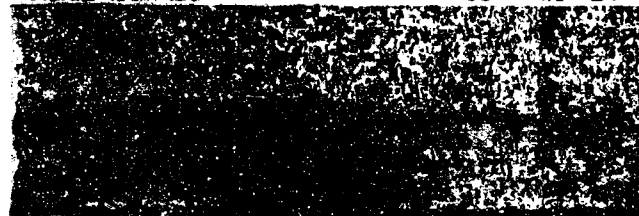
20 OCT 63 00 53 07.2 44.7N 150.7E
KURIL ISLANDS 25 7.0 32



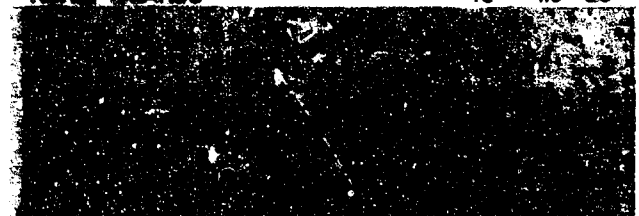
15 OCT 63 12 52 25.3 44.6N 150.5E
KURIL ISLANDS 30 4.6 24



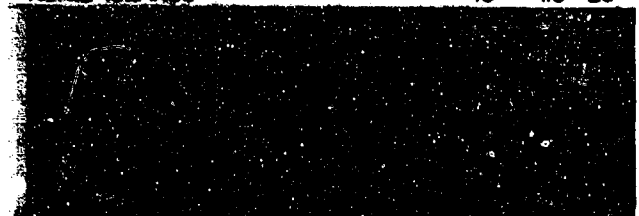
15 OCT 63 08 34 40.1 44.5N 150.9E
KURIL ISLANDS 33 4.5 24



20 OCT 63 02 09 29.4 44.7N 150.0E
KURIL ISLANDS 45 4.9 23



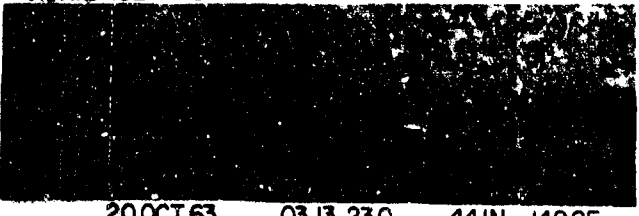
20 OCT 63 01 14 05.2 44.6N 150.1E
KURIL ISLANDS 45 4.8 23



20 OCT 63 04 58 55.0 44.5N 149.7E
KURIL ISLANDS 50 4.4 23



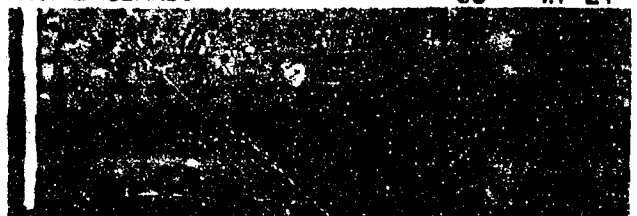
19 OCT 63 00 42 41.9 44.3N 149.7E
KURIL ISLANDS 40 4.0 23



20 OCT 63 03 13 23.0 44.1N 149.8E
KURIL ISLANDS 40 4.3 23



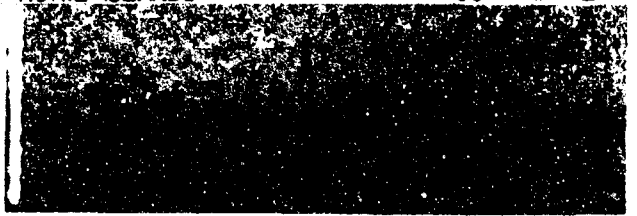
13 OCT 63 01 26 34.3 44.4N 149.3E
KURIL ISLANDS 33 4.4 24



13 OCT 63 01 34 54.3 44.4N 149.2E
KURIL ISLANDS 33 4.4 24



13 OCT 63 04 05 50.1 44.4N 149.2E
KURIL ISLANDS 30 4.4 24



20 OCT 63 03 41 41.9 44.3N 149.4E
KURIL ISLANDS 45 3.9 23



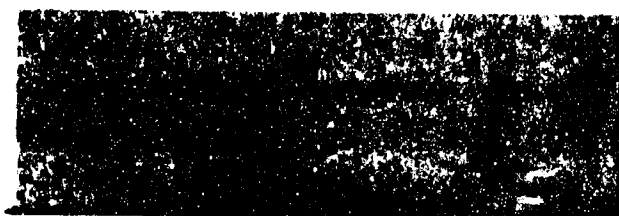
12 OCT 63 23 40 11.1 44.3N 149.2E
KURIL ISLANDS 40 4.3 24



20 OCT 63 01 40 39.5 43.9N 149.8E
KURIL ISLANDS 40 4.2 23



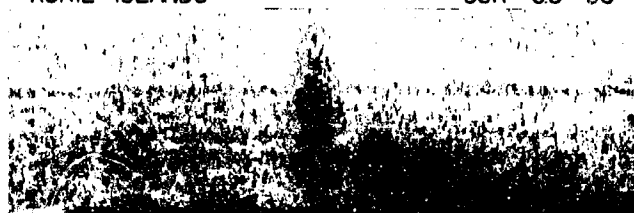
06 JUL 65 06 39 25.0 44.5N 148.3E
KURIL ISLANDS 56 4.4 24



30 JAN 68 03 23 41.9 43.3N 147.4E
KURIL ISLANDS 33R 4.9 23



04 FEB 68 11 06 21.0 43.1N 147.0E
KURIL ISLANDS 35R 5.3 30



04 FEB 68 11 00 50.1 43.0N 147.1E
KURIL ISLANDS 33R 5.5 30



21 APR 67 04 15 51.0 43.3N 146.3E
KURIL ISLANDS 48 4.4 32



30 JAN 68 06 08 35.2 43.5N 147.1E
KURIL ISLANDS 33R 5.0 24



29 JAN 68 16 42 50.4 43.5N 147.2E
KURIL ISLANDS 36R 5.7 24



04 FEB 68 09 10 25.3 43.2N 147.2E
KURIL ISLANDS 33R 5.4 30



30 JAN 68 04 10 36.1 43.1N 147.1E
KURIL ISLANDS 24 5.1 24



10 MAY 68 10 19 32.0 43.6N 145.8E
HOKKAIDO, JAPAN REGION 60R 4.3 43



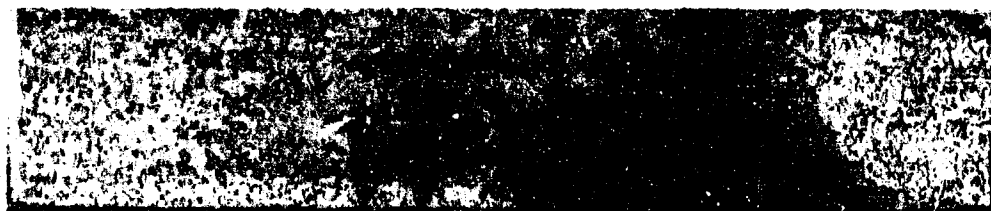
29 MAY 67 21 01 44.3 43.3N 145.7E
HOKKAIDO, JAPAN REGION 88R 5.3 34



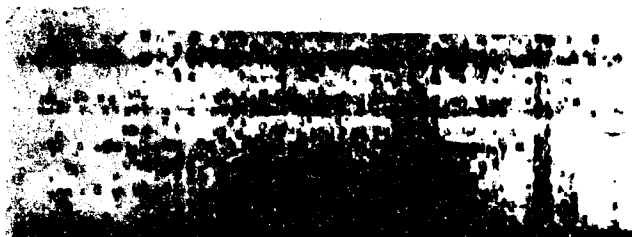
12 MAR 67 02 51 54.7 42.6N 143.0E
HOKKAIDO, JAPAN REGION 33 5.3 23



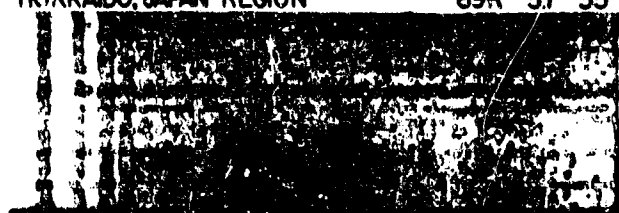
29 JAN 68 10 19 05.6 43.6N 146.7E
KURIL ISLANDS 40 7.0 13



24 JAN 67 03 05 39.0 41.4N 141.9E
HOKKAIDO, JAPAN REGION 69R 57 35



25 FEB 68 13 38 46.4 42.0N 142.4E
HOKKAIDO, JAPAN REGION 72 47 23



26 JUN 68 05 54 24.0 41.2N 142.9E
HOKKAIDO, JAPAN REGION 33R 43 35



05 DEC 66 10 45 02.0 41.9N 141.1E
HOKKAIDO, JAPAN REGION 27 43 32



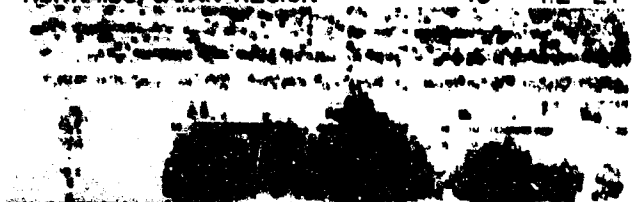
21 JUN 68 13 49 32.5 41.2N 142.4E
HOKKAIDO, JAPAN REGION 33 41 23



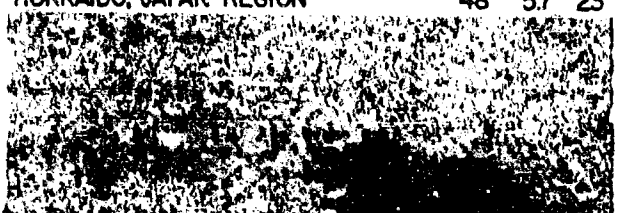
23 JUN 68 04 57 52.2 41.6N 143.4E
HOKKAIDO, JAPAN REGION 45 42 24



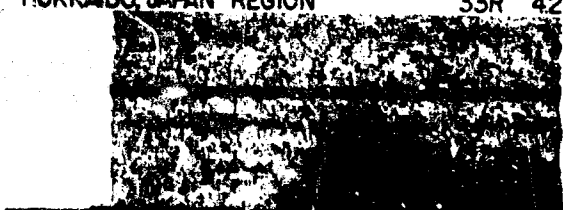
17 JUN 68 11 53 00.4 41.0N 143.0E
HOKKAIDO, JAPAN REGION 48 57 23



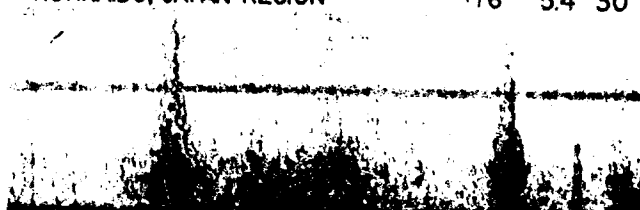
18 JUN 68 07 38 13.0 41.5N 142.9E
HOKKAIDO, JAPAN REGION 33R 42 23



22 FEB 67 16 24 39.1 41.6N 139.7E
HOKKAIDO, JAPAN REGION 176 54 30



20 JUN 68 18 12 25.3 41.4N 142.6E
HOKKAIDO, JAPAN REGION 50 46 23



01 MAY 68 19 16 39.0 40.9N 142.4E
NEAR EAST COAST OF HONSHU, JAPAN 45 47 24



18 JUN 68 17 10 41.8 41.4N 142.5E
HOKKAIDO, JAPAN REGION 34 46 34

16 MAY 68 00 48 55.4 40.8N 143.2E
OFF EAST COAST OF HONSHU, JAPAN 7 7.9 24

02 MAY 68 05 38 48.3 40.7N 142.8E
NEAR EAST COAST OF HONSHU, JAPAN 43 46 35

22 JUN 68 01 12 30.9 40.3N 143.7E
OFF EAST COAST OF HONSHU, JAPAN 15 5.6 34

19 JUN 68 18 03 21.1 40.3N 143.3E
OFF EAST COAST OF HONSHU, JAPAN 33R 4.5 32

19 JUN 68 19 13 01.1 40.3N 143.3E
OFF EAST COAST OF HONSHU, JAPAN 33R 4.1 32

24 MAR 67 04 11 29.6 40.2N 144.6E
OFF EAST COAST OF HONSHU, JAPAN 27 5.0 24

27 JUN 68 21 54 14.1 40.1N 143.8E
OFF EAST COAST OF HONSHU, JAPAN 33R 4.5 23

17 JUN 68 16 56 13.1 40.1N 143.7E
OFF EAST COAST OF HONSHU, JAPAN 6 5.2 22

25 MAY 68 11 52 57.4 40.1N 143.1E
OFF EAST COAST OF HONSHU, JAPAN 37R 5.2 34

28 JUN 68 09 30 29.6 39.9N 143.0E
OFF EAST COAST OF HONSHU, JAPAN 33R 4.5 22

18 JUN 68 08 56 23.7 39.7N 141.8E
HONSHU, JAPAN 33R 4.7 23

25 JUN 68 23 33 18.0 39.6N 143.4E
OFF EAST COAST OF HONSHU, JAPAN 16 5.3 24



28 JUN 68 02 11 14° 39.6N 143.1E
OFF EAST COAST OF HONSHU, JAPAN 33R 4.3 23



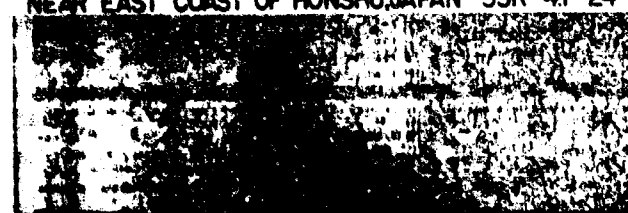
27 JUN 68 23 13 53° 39.4N 142.9E
NEAR EAST COAST OF HONSHU, JAPAN 33R 4.4 23



18 JUN 68 13 38 01° 39.5N 142.4E
NEAR EAST COAST OF HONSHU, JAPAN 33R 4.1 24



12 JUN 68 19 38 43.5 39.3N 142.7E
NEAR EAST COAST OF HONSHU, JAPAN 40 46 34



26 JUN 68 20 26 19.0 39.5N 143.0E
OFF EAST COAST OF HONSHU, JAPAN 34 4.5 35



28 JUN 68 09 44 07.7 39.3N 142.7E
NEAR EAST COAST OF HONSHU, JAPAN 33 4.7 35



12 JUN 68 19 36 24.7 39.5N 143.0E
OFF EAST COAST OF HONSHU, JAPAN 55 46 34



12 JUN 68 21 57 41.3 39.3N 142.8E
NEAR EAST COAST OF HONSHU, JAPAN 36 5.7 34



12 JUN 68 16 23 17.1 39.5N 143.1E
OFF EAST COAST OF HONSHU, JAPAN 21 4.7 34



12 JUN 68 15 48 59.5 39.3N 143.0E
OFF EAST COAST OF HONSHU, JAPAN 30 5.1 32



12 JUN 68 17 23 18° 39.5N 143.1E
OFF EAST COAST OF HONSHU, JAPAN 33R 4.3 34



23 JUN 68 05 20 38.0 39.1N 143.0E
OFF EAST COAST OF HONSHU, JAPAN 45 4.3 24



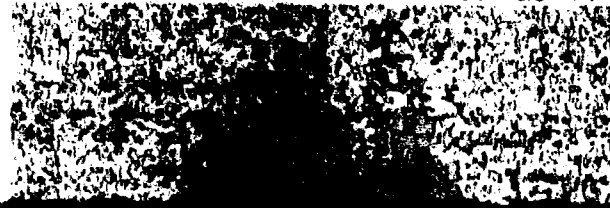
12 JUN 68 19 48 53.4 39.4N 142.8E
NEAR EAST COAST OF HONSHU, JAPAN 33R 4.7 32



12 JUN 68 16 29 13° 39.0N 143.5E
OFF EAST COAST OF HONSHU, JAPAN 33R 4.3 34



01 MAY 68 08 43 474 38.6N 143.1E
OFF EAST COAST OF HONSHU, JAPAN 36 53 44



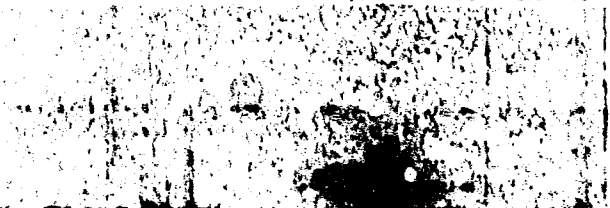
30 DEC 67 02 27 503 38.4N 142.0E
NEAR EAST COAST OF HONSHU, JAPAN 33 43 23



19 FEB 68 14 48 249 38.3N 141.8E
NEAR EAST COAST OF HONSHU, JAPAN 50 43 24



25 FEB 68 20 00 31.5 37.6N 141.4E
NEAR EAST COAST OF HONSHU, JAPAN 66R 55 13



01 NOV 67 19 17 247 37.1N 141.3E
NEAR EAST COAST OF HONSHU, JAPAN 72 47 23



13 NOV 67 10 30 10* 36.8N 140.8E
NEAR EAST COAST OF HONSHU, JAPAN 69 41 24



21 MAR 68 00 40 591 36.0N 140.4E
NEAR EAST COAST OF HONSHU, JAPAN 64 44 32



04 NOV 65 09 19 06* 35.7N 140.8E
NEAR EAST COAST OF HONSHU, JAPAN 81 39 25



26 SEP 67 14 53 14.1 35.5N 140.9E
NEAR EAST COAST OF HONSHU, JAPAN 51 41 32



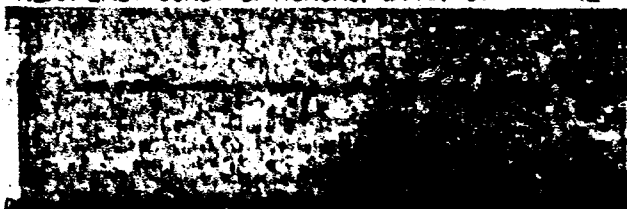
08 NOV 67 01 56 50 35.5N 140.8E
NEAR EAST COAST OF HONSHU, JAPAN 56 43 24



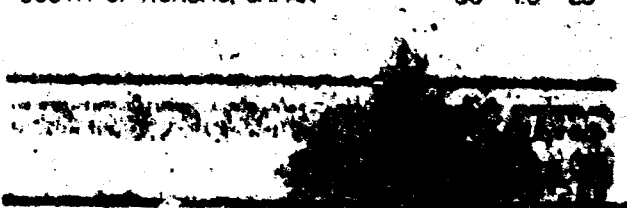
16 MAY 67 05 21 274 34.9N 140.0E
NEAR SOUTH COAST OF HONSHU, JAPAN 44 42 32



01 NOV 67 18 55 34* 34.6N 140.6E
NEAR EAST COAST OF HONSHU, JAPAN 97 42



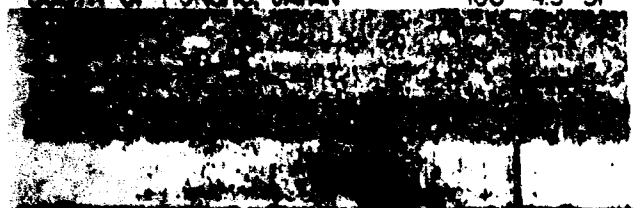
25 JUN 68 04 06 141 32.9N 141.2E
SOUTH OF HONSHU, JAPAN 35 43 23



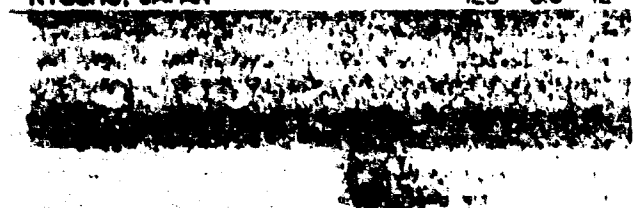
09 JAN 68 13 28 242 31.0N 138.0E
SOUTH OF HONSHU, JAPAN 40 47 24



12 NOV 67 17 13 58.3 30.7N 139.9E
SOUTH OF HONSHU, JAPAN 100 4.5 31



28 NOV 67 02 36 54.1 32.1N 130.8E
KYUSHU, JAPAN 125 5.6 42



27 NOV 67 21 46 02.9 28.5N 129.0E
RYUKYU ISLANDS 17 5.0 42



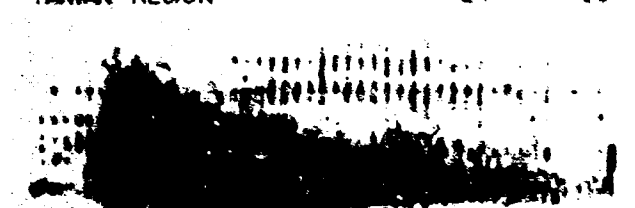
10 MAY 68 15 09 20.6 24.3N 121.9E
TAIWAN 26 4.8 43



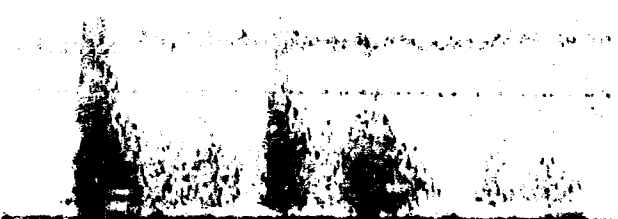
10 MAY 68 09 23 31.5 24.3N 121.8E
TAIWAN 21 4.8 43



16 FEB 68 10 50 16.7 22.7N 121.5E
TAIWAN REGION 24 3.0 30



17 JUN 68 04 26 31.9 22.4N 121.4E
TAIWAN REGION 39 5.1 32



28 MAR 67 19 32 25.4 17.1N 122.4E
LUZON, PHILIPPINE ISLANDS 51 5.3 23



28 MAR 67 21 23 05.6 17.1N 122.6E
LUZON, PHILIPPINE ISLANDS 47 4.4 23



29 JAN 68 16 00 07.3 2.3N 125.5E
SAMAR, PHILIPPINE ISLANDS 51 5.3 24



12 JUN 68 20 15 47.8 0.6S 132.8E
WEST NEW GUINEA REGION 33R 5.6 32



06 FEB 64 08 00 35.0 27.4N 144.3E
BONIN ISLANDS REGION 40 4.6 32

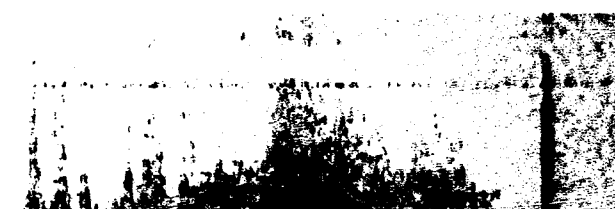


11 AUG 67 18 54 29.8 22.1N 144.0E
VOLCANO ISLANDS REGION 125 5.3 24





19 APR 68 23 40 48° 207N 144E
 MARIANA ISLANDS 3S 49 44



29 MAY 67 04 45 439 119N 1433E
 SOUTH OF MARIANA ISLANDS 33R 56 34



29 APR 67 06 24 590 193N 1462E
 MARIANA ISLANDS REGION 114 48 44



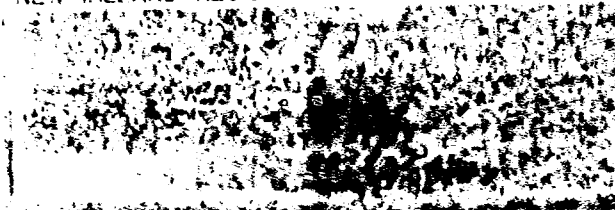
13 MAR 67 04 53 30° 3.2S 1476E
 BISMARK SEA 33R 49 32



12 FEB 69 05 44 476 55S 1532E
 NEW IRELAND REGION 74 1 32



19 APR 68 23 25 439 2N 1438E
 MARIANA ISLANDS 53 44



02 FEB 67 18 15 174 43S 1537E
 NEW IRELAND REGION 267 50 34



18 DEC 67 14 3 95 12N 1436E
 SOUTH OF MARIANA ISLANDS 12 55 32



15 DEC 67 12 04 384 49S 1537E
 NEW IRELAND REGION 104 51 32



07 DEC 66 10 53 252 119N 1476E
 SOUTH OF MARIANA ISLANDS 53 51 32



28 DEC 67 04 28 21* 5.0S 153.7E
NEW IRELAND REGION 130 49 37

29 MAR 64 21 40 32.7 6.7S 155.1E
SOLOMON ISLANDS 68 53 44

28 DEC 67 08 52 42.3 5.1S 153.7E
NEW IRELAND REGION 59 5.2 43

26 SEP 67 17 05 55.0 7.1S 155.8E
SOLOMON ISLANDS 94 57 34

23 DEC 67 01 23 33.6 5.3S 153.7E
NEW IRELAND REGION 64 7.0 43

11 OCT 67 13 14 21.2 5.6S 153.8E
NEW IRELAND REGION 69 4.5 32

10 APR 67 15 02 42.2 7.3S 155.8E
SOLOMON ISLANDS 29R 5.6 32

25 DEC 67 11 41 25* 4.9S 153.9E
NEW IRELAND REGION 95R 4.5 32

10 APR 67 18 24 51.7 7.3S 155.8E
SOLOMON ISLANDS 78 5.3 32

04 OCT 67 17 21 20.7 5.1S 153.9E
NEW IRELAND REGION 52 7 32

18 APR 62 12 49 33* 6.9S 156.0E
SOLOMON ISLANDS 167 5.1 32

21 JAN 68 00 28 12.5 5.2S 154.0E
SOLOMON ISLANDS 113 5.1 23

17 OCT 65 01 53 33.7 8.0S 156.3E
SOLOMON ISLANDS 20 5.6 34

05 JAN 69 13 26 39.9 8.0S 158.9E
SOLOMON ISLANDS 47 64 23

15 SEP 63 01 57 24* 9.4S 167.0E
SANTA CRUZ ISLANDS 33 50 32

15 SEP 63 04 50 21.5 10.2S 165.3E
SANTA CRUZ ISLANDS 31 45 32

15 SEP 63 06 15 21.7 10.2S 165.4E
SANTA CRUZ ISLANDS 28 47 32

15 SEP 63 00 46 54.1 10.3S 165.6E
SANTA CRUZ ISLANDS 43 7 32

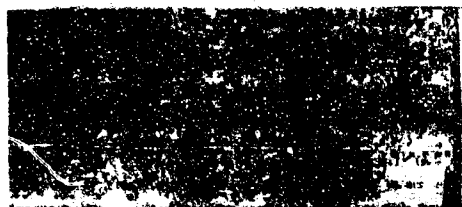
11 JAN 67 03 41* 11.3S 165.6E
SANTA CRUZ ISLANDS 33 45 24

29 JUL 65 07 06 12.9 11.7S 166.2E
SANTA CRUZ ISLANDS 80 47 24

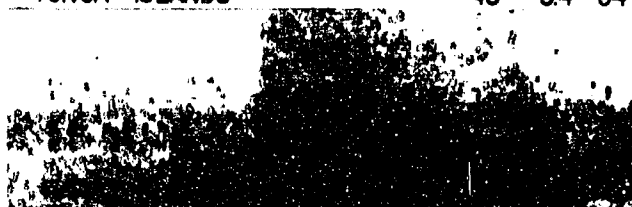
04 DEC 66 04 56 58.2 140S 167.1E
NEW HEBRIDES ISLANDS 132 6.1 24



16 OCT 65 22 14 15.1 15.2S 173.5W
TONGA ISLANDS 45 5.4 34



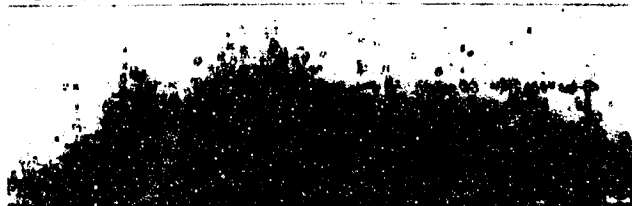
14 AUG 65 00 29 01.7 16.6S 167.9E
NEW HEBRIDES ISLANDS 50 4.3 24



08 JAN 68 21 54 20.8 14.8S 174.8W
SAMOA ISLANDS REGION 16 5.5 43



13 AUG 65 20 07 35.7 16.7S 167.9E
NEW HEBRIDES ISLANDS 33 4.9 25



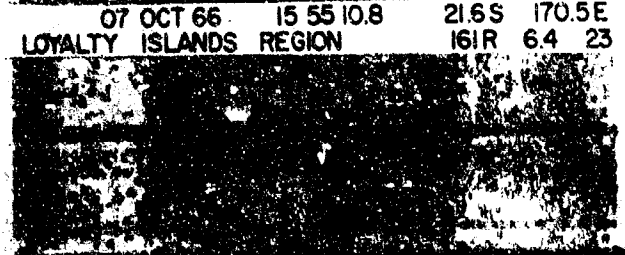
20 APR 68 12 25 10.1 15.7S 172.6W
SAMOA ISLANDS REGION 30 5.7 23



07 OCT 66 15 55 10.8 21.6S 170.5E
LOYALTY ISLANDS REGION 161R 6.4 23



28 APR 68 14 08 57.9 19.5S 155.5W
HAWAII 27 4.7 44



26 JUN 65 15 40 31.1 22.2S 171.4E
LOYALTY ISLANDS REGION 90 5.6 22



09 JAN 68 00 25 42* 15.4S 174.5W
TONGA ISLANDS 52 4.6 43

DOCUMENT CONTROL DATA - R&D

(Security classification of title, body of abstract and indexing annotation must be entered when the overall report is classified)

1. ORIGINATING ACTIVITY (Corporate author) Hawaii Institute of Geophysics University of Hawaii Honolulu, Hawaii 96822		2a. REPORT SECURITY CLASSIFICATION Unclassified	
3. REPORT TITLE <u>T-Wave</u> Generation Mechanisms		2b. GROUP	
4. DESCRIPTIVE NOTES (Type of report and inclusive dates)			
5. AUTHOR(S) (Last name, first name, initial) Johnson, Rockne H. and Norris, Roger A.			
6. REPORT DATE January 1970	7a. TOTAL NO. OF PAGES 59	7b. NO. OF REFS 20	
8a. CONTRACT OR GRANT NO. Contract No. Nonr-3748(01)	9a. ORIGINATOR'S REPORT NUMBER(S) HIG-70-7		
b. PROJECT NO. Project Code 8100	9b. OTHER REPORT NO(S) (Any other numbers that may be assigned to this report) None		
10. AVAILABILITY/LIMITATION NOTICES No limitation			
11. SUPPLEMENTARY NOTES		12. SPONSORING MILITARY ACTIVITY Advanced Research Projects Agency	
13. ABSTRACT <p>The transformation of earthquake body waves to <u>T</u> waves is as efficient at deep slopes as at slopes which transect the sofar axis. Moreover, spectral studies of <u>T</u> phase signatures have shown no basis for distinguishing between the two cases. As simple downslope propagation is inadequate to explain the production of <u>T</u> waves at deep slopes, that process is relegated a minor role in favor of scattering from the sea floor as the dominant mechanism. A slope in the direction of propagation insures that once energy is scattered in that direction the probability of its being unfavorably rescattered upon successive approaches to the sea floor will be less. Scattering near the sea surface is detectable in the absence of bottom-scattered <u>T</u> waves. Such abyssally generated <u>T</u> waves display a distinctly higher frequency spectrum when originating in subarctic regions than when originating in lower latitudes. This difference is ascribed to downward ducting of higher frequency energy from the subarctic surface channel.</p>			

Unclassified

Security Classification

KEY WORDS

LINK A

LINK B

LINK C

ROLE

WT

ROLE

WT

ROLE

WT

T-wave Generation Mechanisms

INSTRUCTIONS

1. **ORIGINATING ACTIVITY:** Enter the name and address of the contractor, subcontractor, grantee, Department of Defense activity or other organization (corporate author) issuing the report.

2a. **REPORT SECURITY CLASSIFICATION:** Enter the overall security classification of the report. Indicate whether "Restricted Data" is included. Marking is to be in accordance with appropriate security regulations.

2b. **GROUP:** Automatic downgrading is specified in DoD Directive 5200.10 and Armed Forces Industrial Manual. Enter the group number. Also, when applicable, show that optional markings have been used for Group 3 and Group 4 as authorized.

3. **REPORT TITLE:** Enter the complete report title in all capital letters. Titles in all cases should be unclassified. If a meaningful title cannot be selected without classification, show title classification in all capitals in parentheses immediately following the title.

4. **DESCRIPTIVE NOTES:** If appropriate, enter the type of report, e.g., interim, progress, summary, annual, or final. Give the inclusive dates when a specific reporting period is covered.

5. **AUTHOR(S):** Enter the name(s) of author(s) as shown on or in the report. Enter last name, first name, middle initial. If military, show rank and branch of service. The name of the principal author is an absolute minimum requirement.

6. **REPORT DATE:** Enter the date of the report as day, month, year; or month, year. If more than one date appears on the report, use date of publication.

7a. **TOTAL NUMBER OF PAGES:** The total page count should follow normal pagination procedures, i.e., enter the number of pages containing information.

7b. **NUMBER OF REFERENCES:** Enter the total number of references cited in the report.

8a. **CONTRACT OR GRANT NUMBER:** If appropriate, enter the applicable number of the contract or grant under which the report was written.

8b, 8c, & 8d. **PROJECT NUMBER:** Enter the appropriate military department identification, such as project number, subproject number, system numbers, task number, etc.

9a. **ORIGINATOR'S REPORT NUMBER(S):** Enter the official report number by which the document will be identified and controlled by the originating activity. This number must be unique to this report.

9b. **OTHER REPORT NUMBER(S):** If the report has been assigned any other report numbers (either by the originator or by the sponsor), also enter this number(s).

10. **AVAILABILITY/LIMITATION NOTICES:** Enter any limitations on further dissemination of the report, other than those

imposed by security classification, using standard statements such as:

- (1) "Qualified requesters may obtain copies of this report from DDC."
- (2) "Foreign announcement and dissemination of this report by DDC is not authorized."
- (3) "U. S. Government agencies may obtain copies of this report directly from DDC. Other qualified DDC users shall request through _____."
- (4) "U. S. military agencies may obtain copies of this report directly from DDC. Other qualified users shall request through _____."
- (5) "All distribution of this report is controlled. Qualified DDC users shall request through _____."

If the report has been furnished to the Office of Technical Services, Department of Commerce, for sale to the public, indicate this fact and enter the price, if known.

11. **SUPPLEMENTARY NOTES:** Use for additional explanatory notes.

12. **SPONSORING MILITARY ACTIVITY:** Enter the name of the departmental project office or laboratory sponsoring (paying for) the research and development. Include address.

13. **ABSTRACT:** Enter an abstract giving a brief and factual summary of the document indicative of the report, even though it may also appear elsewhere in the body of the technical report. If additional space is required, a continuation sheet shall be attached.

It is highly desirable that the abstract of classified reports be unclassified. Each paragraph of the abstract shall end with an indication of the military security classification of the information in the paragraph, represented as (TS), (S), (C), or (U).

There is no limitation on the length of the abstract. However, the suggested length is from 150 to 225 words.

14. **KEY WORDS:** Key words are technically meaningful terms or short phrases that characterize a report and may be used as index entries for cataloging the report. Key words must be selected so that no security classification is required. Identifiers, such as equipment model designation, trade name, military project code name, geographic location, may be used as key words but will be followed by an indication of technical context. The assignment of links, roles, and weights is optional.

Unclassified